AMERICAN SOCIETY FOR MICROBIOLOGY | Journal of Bacteriology®

RESEARCH ARTICLE

Light Modulates Important Pathogenic Determinants and Virulence in ESKAPE Pathogens *Acinetobacter baumannii*, *Pseudomonas aeruginosa*, and *Staphylococcus aureus*

M. R. Tuttobene,[a] J. F. Pérez,[b] E. S. Pavesi,[a] B. Perez Mora,[a] D. Biancotti,[a] P. Cribb,[c] M. Altilio,[a] G. L. Müller,[a] H. Gramajo,[c] G. Tamagno,[d] M. S. Ramírez,[e] L. Diacovich,[c] M. A. Mussi[a]

[a]Centro de Estudios Fotosintéticos y Bioquímicos (CEFOBI-CONICET), Rosario, Argentina
[b]Facultad de Ciencias Bioquímicas y Farmacéuticas, Universidad Nacional de Rosario, Rosario, Argentina
[c]Instituto de Biología Celular y Molecular de Rosario (IBR-CONICET), Ocampo y Esmeralda, Rosario, Argentina
[d]Hospital Provincial del Centenario, Rosario, Argentina
[e]Department of Biological Science, California State University, Fullerton, Fullerton, California, USA

M. R. Tuttobene, J. F. Pérez, and E. Pavesi contributed equally to this work. The order of authors was determined according to increasing seniority.

ABSTRACT Light sensing has been extensively characterized in the human pathogen *Acinetobacter baumannii* at environmental temperatures. However, the influence of light on the physiology and pathogenicity of human bacterial pathogens at temperatures found in warm-blooded hosts is still poorly understand. In this work, we show that *Staphylococcus aureus*, *Acinetobacter baumannii*, and *Pseudomonas aeruginosa* (ESKAPE) priority pathogens, which have been recognized by the WHO and the CDC as critical, can also sense and respond to light at temperatures found in human hosts. Most interestingly, in these pathogens, light modulates important pathogenicity determinants as well as virulence in an epithelial infection model, which could have implications in human infections. In fact, we found that alpha-toxin-dependent hemolysis, motility, and growth under iron-deprived conditions are modulated by light in *S. aureus*. Light also regulates persistence, metabolism, and the ability to kill competitors in some of these microorganisms. Finally, light exerts a profound effect on the virulence of these pathogens in an epithelial infection model, although the response is not the same in the different species; virulence was enhanced by light in *A. baumannii* and *S. aureus*, while in *A. nosocomialis* and *P. aeruginosa* it was reduced. Neither the BlsA photoreceptor nor the type VI secretion system (T6SS) is involved in virulence modulation by light in *A. baumannii*. Overall, this fundamental knowledge highlights the potential use of light to control pathogen virulence, either directly or by manipulating the light regulatory switch toward the lowest virulence/persistence configuration.

IMPORTANCE Pathogenic bacteria are microorganisms capable of producing disease. Dangerous bacterial pathogens, such as *Staphylococcus aureus*, *Pseudomonas aeruginosa*, and *Acinetobacter baumannii*, are responsible for serious intrahospital and community infections in humans. Therapeutics is often complicated due to resistance to multiple antibiotics, rendering them ineffective. In this work, we show that these pathogens sense natural light and respond to it by modulating aspects related to their ability to cause disease; in the presence of light, some of them become more aggressive, while others show an opposite response. Overall, we provide new understanding on the behavior of these pathogens, which could contribute to the control of infections caused by them. Since the response is distributed in diverse pathogens, this notion could prove a general concept.

KEYWORDS ESKAPE pathogens, cell motility, hemolysis, light regulation, virulence

Citation Tuttobene MR, Pérez JF, Pavesi ES, Perez Mora B, Biancotti D, Cribb P, Altilio M, Müller GL, Gramajo H, Tamagno G, Ramírez MS, Diacovich L, Mussi MA. 2021. Light modulates important pathogenic determinants and virulence in ESKAPE pathogens *Acinetobacter baumannii*, *Pseudomonas aeruginosa*, and *Staphylococcus aureus*. J Bacteriol 203:e00566-20. https://doi.org/10.1128/JB.00566-20.

Editor George O'Toole, Geisel School of Medicine at Dartmouth

Address correspondence to L. Diacovich, diacovich@ibr-conicet.gov.ar, or M. A. Mussi, mussi@cefobi-conicet.gov.ar.

Received 13 October 2020
Accepted 3 December 2020
Accepted manuscript posted online 7 December 2020
Published 8 February 2021

The advances in medicine during the last 70 years have been catalyzed by the ability that antimicrobial agents offer to control infections (1, 2). However, the rapid evolution of multidrug- and extensively drug-resistant (MDR and XDR, respectively) bacteria, which render the drugs ineffective (2), awaked a major challenge for the near future. The situation has been worsened by the scarce release of new antimicrobial agents into the market (3, 4). Alternatives to control bacterial infections are thus urgently required.

Enterococcus faecium, *Staphylococcus aureus*, *Klebsiella pneumoniae*, *Acinetobacter baumannii*, *Pseudomonas aeruginosa*, and *Enterobacter* species (ESKAPE) pathogens have growing multidrug resistance and virulence (5), are responsible for the majority of nosocomial infections, and are capable of "escaping" the biocidal action of antimicrobial agents (2, 5). ESKAPE pathogens are associated with high mortality and morbidity rates, high health care costs, diagnostic dilemma, and difficulty in the initiation of empirical treatment (4, 6). In particular, *S. aureus* is a natural resident of the skin and nasal membranes with an alarming pathogenic potential to cause a variety of community- and hospital-acquired infections (7). It is simultaneously the leading cause of bacteremia and infective endocarditis (IE) and can also cause pleuropulmonary, osteoarticular, skin, and soft tissue infections (7). *S. aureus* is a prominent wound pathogen, capable of both acute and chronic infections upon the formation of biofilms (8). Methicillin-resistant *S. aureus* (MRSA) USA300 and closely related variants are now the most prevalent community-acquired MRSA (CA-MRSA) isolates in North America and northern regions of South America (3). A crucial factor that allows the spread of *S. aureus* in hospitals and communities is its ability to resist desiccation (9). *A. baumannii* infections typically occur in hospitalized patients or patients with significant contact with the health care system. Although *A. baumannii* infection rates are comparatively low compared with those of other ESKAPE pathogens (3), approximately 45% of all global *A. baumannii* isolates are considered MDR (3). These levels of MDR are four times higher than those observed for *P. aeruginosa* or *K. pneumoniae*. A key aspect of *A. baumannii*'s physiology is its propensity to develop rapid resistance to antibiotics, as well as its outstanding ability to persist in the environment, which contributes to the spread of resistant clones (8). Due to the increasing and fast development of resistance to routinely applied antibiotics, this pathogen is widely responsible for skin, skin wound, soft tissue, bloodstream, respiratory, and urinary infections, especially in intensive care units (8). Serious infections from *P. aeruginosa* generally occur only in health care (nosocomial) settings, but people can also develop mild infections in other environments. Common hospital-associated *P. aeruginosa* infections include bloodstream, pneumonia (lung infection), urinary tract, and surgical wound infections, as well as respiratory infections in patients with cystic fibrosis. The plasticity and adaptability of the *P. aeruginosa* genome are key features in the pathogen's ability to chronically persist in the host and evade antibiotic treatment (3).

Some years ago, a new physiological trait was recognized in *A. baumannii*, namely, its ability to sense and respond to light-modulating aspects related to bacterial persistence at environmental temperatures (10). In fact, we have shown that light modulates iron uptake; motility; tolerance to antibiotics; antibiotic susceptibility; killing of competitors; antioxidant enzyme production, such as catalase; phenylacetic acid and acetoin catabolism; biofilm formation; and trehalose metabolism at environmental temperatures (10–16). Photoregulation of many of these traits is governed by the blue-light using flavin adenine dinucleotide (BLUF)-type photoreceptor BlsA, which is functional in the low to moderate temperature range (18°C to 24°C) (10, 17, 18). BlsA is a global regulator that interacts with and antagonizes the functioning of transcriptional regulators, such as Fur, or AcoN repressors, inducing expression of their target genes only in the dark or in the presence of blue light, respectively (15, 16). BlsA is thus a photoreceptor that signals not only under blue light but also in the dark and superimposes a second-order regulation upon traditional transcriptional regulation (12, 15, 16). The presence of another "nontraditional" photoregulator modulating antibiotic susceptibility

has also been suggested in *A. baumannii* (13, 14). Moreover, light sensing is distributed within the *Acinetobacter* genus and not restricted to *A. baumannii* (19).

Since many physiological traits were found to be modulated by light at environmental temperatures, we wondered whether light can also exert an influence at temperatures found in warm-blooded animals, which could have implications in human infections. In this work, we studied the effect of light on pathogenicity determinants of Gram-negative and -positive ESKAPE pathogens at 37°C. *Acinetobacter nosocomialis*, which belongs to the *Acinetobacter calcoaceticus-A. baumannii* complex (20), was also included in this study, as it is an important nosocomial pathogen whose incidence has been underestimated in clinical settings (21). We show that light modulates alpha-toxin-dependent hemolysis in *S. aureus*, which is a key virulence determinant in this microorganism since its pathogenicity relies on the ability to damage the host cell membrane with toxins and peptides (22). Interestingly, light also modulates different metabolic traits, including growth under iron deprivation conditions, acetoin and phenyl-acetic acid (PAA) catabolism (23), and trehalose utilization in many of these pathogens. Importantly, virulence is significantly modulated by light in *A. baumannii*, *A. nosocomialis*, *P. aeruginosa*, and *S. aureus* in an epithelial infection model using a human keratinocyte cell line. Light enhances virulence in *S. aureus* and *A. baumannii*, while the opposite effect occurs in *P. aeruginosa* and *A. nosocomialis*, thus indicating that the response to light is species specific and likely related to the pathophysiology developed by each pathogen. Overall, this work not only introduces novel concepts regarding the biology of important ESKAPE pathogens, such as light sensing in *S. aureus* and *P. aeruginosa* at 37°C, but also provides evidence suggesting that the light regulatory switch could be a potential target to control infections caused by ESKAPE pathogens. The facts that visible light is an economic, accessible, and ubiquitous signal and also that the doses and intensity used in these experiments are very low and do not affect host cell viability make exposure to this stimulus a feasible approach to help treat ESKAPE infections.

RESULTS

Light modulates hemolysis in *S. aureus* at 37°C. Since hemolysis is an important virulence determinant influencing pathogenesis in *S. aureus*, we studied whether blue light modulates this trait at 37°C.

The effect of blue light on hemolysis was analyzed by using different *S. aureus* clinical isolates recovered from a public hospital located in Rosario, Santa Fe, Argentina (see Table S1 in the supplemental material), in addition to the model strains RN4220 (24) and USA300 (25). To determine the effect of light on hemolysis, 10 μl of overnight-grown cultures (optical density at 660 nm [OD_{660}], 2.5) were spotted onto sheep blood agar plate pairs and incubated under blue light or in the dark at 37°C for 48 h. Our results show that clinical isolates SAU064, SAU356-2, and SAU152 exhibited higher hemolytic levels under the dark than under light conditions (Fig. 1A to C, respectively), as the area of the zone of clearance was approximately 3.2-, 1.5-, and 2.4-fold higher in the dark than in the presence of blue light (Fig. 1H). Isolate SAU207 showed comparable hemolysis levels under light or dark conditions, (i.e., did not show modulation by light) (Fig. 1D and H), while SAU214 did not show hemolysis in the dark nor in the presence of blue light (Fig. 1E). Modulation of hemolysis by light was not related to any particular site of isolation, as was observed in isolates recovered from peripheral venous catheter tip (SAU064), blood culture (SAU356-2), or urine culture (SAU152) (Table S1).

The extensively characterized strain RN4220 (24), which is a mutant in the accessory gene regulator (*agr*) and does not produce α-hemolysin (24), did not show differences between light and dark on sheep blood agar plates (Fig. 1F). In contrast, USA300 showed a marked response to light (Fig. 1G), as the area of the zone of clearance was determined to be 3.5-fold higher in the dark than under blue light at 37°C (Fig. 1H).

As controls, *S. aureus* USA300 cells were lifted from blood agar plates incubated under blue light or in the dark for 48 h (see Fig. S1A in the supplemental material) and

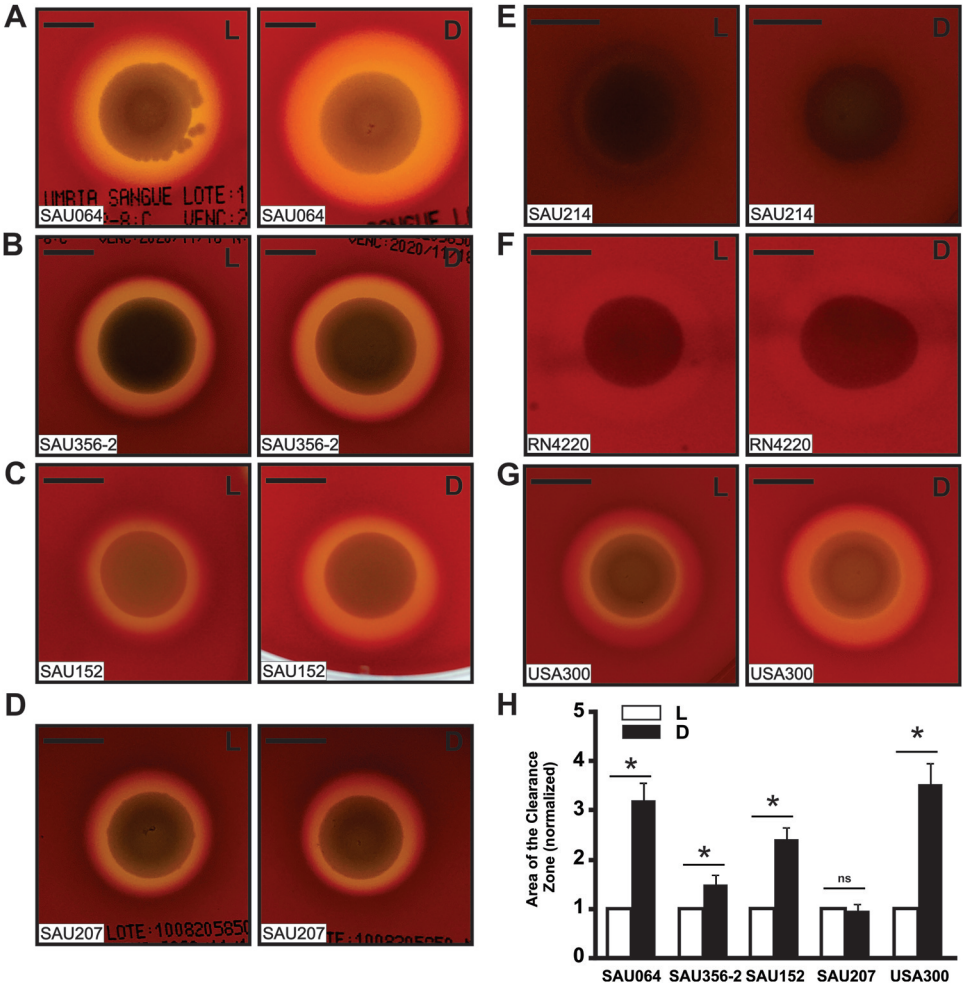

FIG 1 Light modulates hemolysis in *S. aureus* at 37°C. (A to E) Effect of light on hemolysis of five clinical isolates of *S. aureus* SAU064, SAU356-2, SAU152, SAU207, and SAU214, recovered from patients from a public hospital in Rosario, Argentina (Table S1). Also included are the model strains RN4220 (F) and USA300 (G). Sheep blood agar commercial plate pairs were inoculated with 10 μl of the indicated cultures grown to an optical density at 660 nm (OD_{660}) of 2.5. Plates were inspected and photographed after incubation under blue light or in the dark at 37°C for 48 h. Bars represent 7.5 mm. Representative results of at least three independent experiments are shown. (H) Quantification of the area of the zone of clearance in hemolysis plates incubated under blue light (L) or in the dark (D). The area of the zone of clearance was determined as the difference between the area of the hemolytic halo and the area of the bacterial spot, measured using ImageJ software (NIH). The values were normalized to the light condition, which received the arbitrary value of 1. The data presented are the means of at least three independent experiments, and error bars show the standard deviation of the mean. Asterisks indicate significant differences between light and dark treatments, as determined by *t* test ($P < 0.05$). ns, not significant.

resuspended in tryptic soy broth (TSB) medium. Bacterial growth was determined by OD measurement at 660 nm, and no significant differences between light and dark conditions were observed (data not shown). The bacteria were then diluted and counted by plating in tryptic soy agar (TSA) medium at 37°C. No significant differences were observed in the number of bacteria recovered from the plates incubated either under blue light or in the dark (Fig. S1B). Also, we evaluated the effect of light on the size of single colonies (Fig. S1C to E). For this purpose, *S. aureus* USA300 cells were grown overnight on TSB at 37°C and diluted and plated in TSA to determine the titer of single colonies. The plates were then incubated at 37°C in the presence of light or in the dark for 24 hours (Fig. S1C). The results show no significant differences either in the number of colonies (Fig. S1D) or in the size of the single colonies (Fig. S1E) recovered after incubation under blue light or in the dark. The overall results indicate that the effect of light observed on hemolysis is not a consequence of more robust growth of the bacteria in the dark.

In summary, the experimental evidence indicates that light modulates hemolysis in some *S. aureus* strains at 37°C and suggests a wide distribution of the light response phenotype in this species.

Light modulates *hla*-dependent hemolysis. *S. aureus* α-hemolysin (Hla or alpha-toxin), a 33.2-kDa polypeptide encoded by the *hla* gene, is a pore-forming cytotoxin produced by the majority of *S. aureus* strains and targets a broad range of host cell types (7). Like most staphylococcal extracellular proteins, alpha-toxin is not expressed constitutively, but it is tightly regulated by an array of extracellular and intracellular signals (7). α-Hemolysin is the key virulence factor emerging from *in vivo* studies (22).

To study whether light modulates hemolysis through the alpha-toxin, we analyzed the effect of light on an *hla* mutant, as well as on this *hla* mutant harboring plasmid pAH5, from which a wild-type copy of the *hla* gene is expressed by its own promoter (26). Our results show that the *hla* mutant lost the ability to hemolyze on sheep blood agar plates both under blue light and in the dark at 37°C (Fig. 2B). Conversely, the *hla* mutant complemented with a wild-type copy of the *hla* gene (26) restored hemolysis. Moreover, higher levels of hemolysis, approximately 2.3-fold, were observed in the dark than in the light, again showing regulation by light (Fig. 2C and D). Interestingly, the levels of hemolysis in this strain were higher than in the wild-type strain, both under blue light and in the dark (Fig. 1A and C and D). This finding is not surprising and most likely results from an *hla* gene dosage effect, as this gene is present in a high copy number plasmid (27), rather than from a single chromosomal copy. Consistent with the above results, *hla* transcript levels were found to be approximately 5-fold higher in the dark than under light conditions in the wild-type *S. aureus* USA300 strain (Fig. 2E). Overall, our results thus indicate that light regulates *hla*-dependent hemolysis in *S. aureus* at 37°C.

Finally, we observed no hemolysis in the *agrA*, *agrB*, and *agrC* mutants either under blue light or in the dark and no differences in hemolysis in the *saeR* and *sarA* mutants between light and dark (see Fig. S2 in the supplemental material). These regulatory loci code for the staphylococcal accessory protein effector (*sae*), which together with *agr* coordinately control *hla* expression in *S. aureus* (28).

Light modulates motility in *S. aureus* and *P. aeruginosa*. To further study the effect of light on *S. aureus* physiology, another pathogenicity determinant such as motility was assayed at 37°C, as it was previously shown to be modulated by light in other organisms (10). *S. aureus* strain USA300 as well as the clinical isolate SAU152, which showed modulation of hemolysis by light (Fig. 1), were included. As shown in Fig. 3A, *S. aureus* strain USA300 moved away from the inoculation point covering whole motility plates when incubated overnight at 37°C in the dark, while the motility was inhibited in the presence of blue light. In SAU152, motility was inhibited in the presence of light, while the bacteria moved significantly in the dark despite that they did not cover the whole plate (Fig. 3B), also showing that in this strain, motility is modulated by light. The model strain *P. aeruginosa* PAO1, as well as the clinical isolate PAE4840 (Table S1), were also included in this study, as this is also an important pathogen causing severe skin and soft tissue infections. Our results show that the bacteria grew confined to the inoculation point under blue light, while they moved throughout the plate in the dark (Fig. 3C and D, respectively). Overall, our results show that light modulates motility in *S. aureus* and *P. aeruginosa* at 37°C. It should be mentioned that motility is not modulated by light in *A. baumannii* at 37°C (10, 17), while it has been shown to be photoregulated in *A. nosocomialis* at 37°C (19).

Light modulates growth under iron deprivation conditions in *S. aureus*, *P. aeruginosa*, and *A. nosocomialis*. Iron is known to be a limiting nutrient during infections in warm-blooded hosts, and the ability of the bacteria to acquire this metal is essential for the success of a bacterial infection (22, 29). We have previously shown that light modulates iron uptake in *A. baumannii* at environmental temperatures (15). Here, we evaluated whether growth under iron-deprived conditions is modulated by light in these important pathogens at temperatures found in warm-blooded hosts, such as 37°C. In contrast to the response observed for *A. baumannii* at environmental

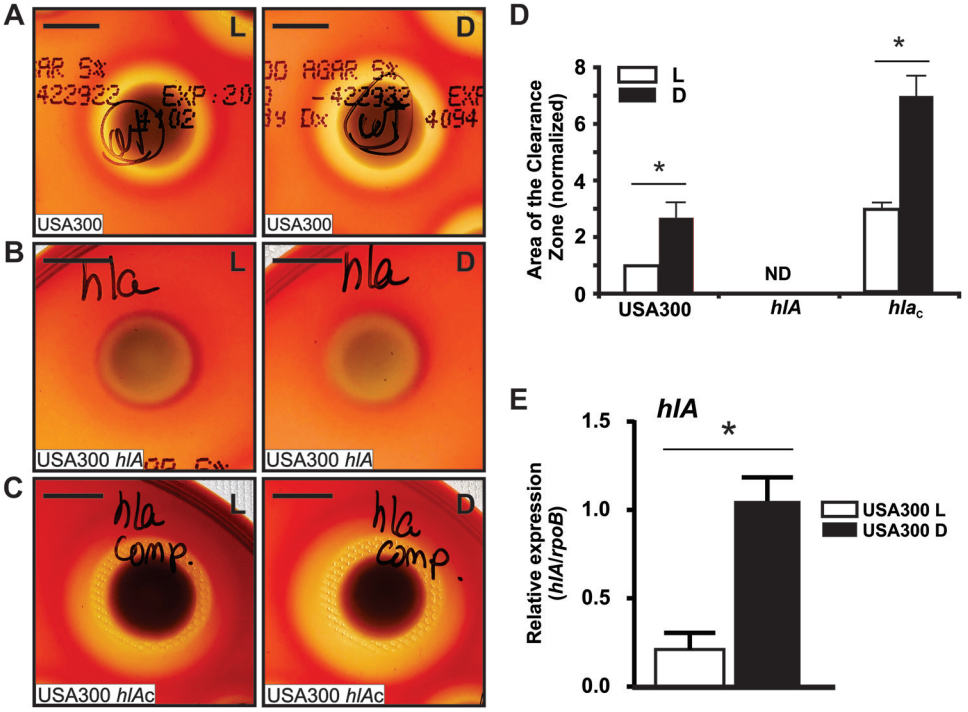

FIG 2 Light modulation of hemolysis depends on alpha-toxin. (A to C) Sheep blood agar plate pairs were inoculated with 10 μl of the following *S. aureus* cultures grown to an OD_{660} of 2.5: *S. aureus* USA300 (A), the isogenic *hla* mutant (B), or the *hla* mutant harboring a wild-type copy of the *hla* gene cloned into plasmid pAH5 (C). Plates were inspected and photographed after incubation under blue light or in the dark at 37°C for 48 hours. Bars represent 7.5 mm. Representative results of at least three independent experiments are shown. (D) Quantification of the area of the clearance zone in hemolysis plates under blue light (L) or in the dark (D). The area of the zone of clearance was determined as the difference between the area of the hemolytic halo and the area of the bacterial spot measured using ImageJ (NIH). The values were normalized to the wild-type strain under light conditions, which received the arbitrary value of 1. The data presented are the means of at least three independent experiments, and error bars show the standard deviation of the mean. Asterisks indicate significant differences between light and dark treatments, as determined by *t* test ($P < 0.05$). ND, not determined. (E) Estimation of the expression levels of *hla* in *S. aureus* USA300 cells grown under blue light (L) or in the dark (D) on sheep blood agar plates for 48 hours at 37°C, by qRT-PCR. Shown are the means from three independent experiments. The *y* axis refers to the fold difference of *hla* to the threshold cycle (C_T) values corresponding to *rpoB*; the standard deviation (SD) is shown. Asterisks indicate significant differences between light and dark treatments, as determined by *t* test ($P < 0.05$).

temperatures, more robust growth resulted under blue light in the presence of the iron chelator 2,2′-dipyridyl (DIP) (iron-deprived conditions) in *S. aureus*, *P. aeruginosa*, and *A. nosocomialis*, while it was severely affected in the dark at 37°C (Fig. 4A, C and E, respectively, and Fig. S3A in the supplemental material). No effect of light was observed on bacterial growth under iron replete conditions, as growth curves were similar under blue light or in the dark for the different strains in LB (Fig. 4B, D, and F). Besides, no light sensitivity was observed for DIP under the experimental conditions used in these experiments (see Fig. S4 in the supplemental material). In the case of *A. baumannii*, we did not observe modulation by light of this trait at 37°C, either for ATCC 17978 or for ATCC 19606 or Ab33405 strains (only ATCC 19606 shown in Fig. 4G). Overall, our results show that growth under iron-limiting conditions is modulated by light in *S. aureus*, *P. aeruginosa*, and *A. nosocomialis* at 37°C.

Light modulates metabolism in *A. nosocomialis* and *S. aureus* at 37°C. Bacterial pathogenesis studies are mainly focused on virulence factors; however, pathogens must adapt their metabolism in order to interact with and survive within the host cells or persist in the environment. Modulation of the PAA catabolic pathway by GacAS, a two-component system composed of a sensor kinase (GacS) and a response regulator (GacA), has been shown to influence *A. baumannii* pathogenesis. In fact, inhibition of this pathway resulted in increased neutrophil migration to the site of infection and

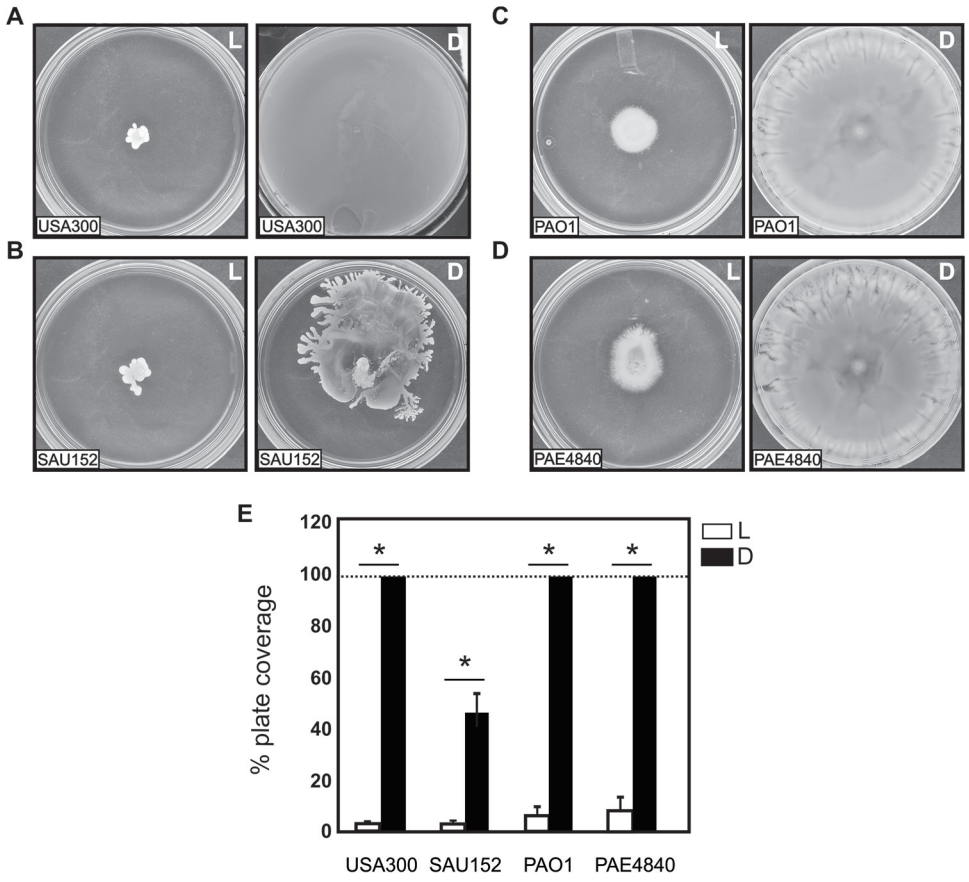

FIG 3 Light modulates motility in *S. aureus* and *P. aeruginosa*. (A to D) Cells of *S. aureus* USA300 (A), the clinical isolate SAU152 (B), *P. aeruginosa* PAO1 (C), and the clinical isolate PAE4840 (D) were inoculated on the surface of swimming plates (see Materials and Methods for descriptions). Plates were inspected and photographed after overnight incubation (24 hours) in darkness (D) or in the presence of blue light (L) at 37°C. The experiments were repeated three times for each strain, and representative results are shown. (E) Quantification of cell motility of the indicated strains estimated as the percentage of plate coverage, i.e., the percentage of the petri plate area covered with bacteria. The area of coverage was measured with ImageJ (NIH). The mean and standard deviation from two independent experiments are provided. For those conditions at which the bacteria reached the edge of the plate, a value of 100% is provided (dotted line). Asterisks indicate significant differences in light compared with dark conditions, as indicated by *t* test ($P < 0.05$).

bacterial clearance (23, 30). Acetoin and 2,3-butanediol (BD), referred as bacterial volatile compounds (BVCs), can mediate cross-kingdom interactions with fungi, plants, and animals and can even modulate antibiotic resistance, biofilm formation, and virulence (31). PAA and acetoin catabolism have been shown to be modulated by light in *A. baumannii* at environmental temperatures through the BlsA photoreceptor (11, 16). PAA catabolism was shown to be repressed by light (11), while acetoin catabolism was found to be stimulated by light in *A. baumannii* at 23°C (16). We have disclosed the mechanism of light signal transduction by showing that the photoreceptor BlsA antagonizes the functioning of the acetoin catabolic repressor AcoN in a temperature-dependent manner (16). In this work, we evaluated the effect of light on these traits in *A. nosocomialis* and *A. baumannii* at 37°C. Our results show that light reduces the ability of *A. nosocomialis* RUH2624 to grow in minimal media with PAA as the sole carbon source at 37°C, while growth was stimulated in the dark (Fig. 5A). On the contrary, no significant differences between light and dark were observed in growth curves on PAA as the sole carbon source for *A. baumannii* ATCC 17978, ATCC 19606, or Ab33405 strains at 37°C (only shown for ATCC 19606 in Fig. 5B). Furthermore, acetoin catabolism was also found to be modulated by light in *A. nosocomialis* RUH2624 at 37°C, as growth on minimal media with acetoin as the sole carbon source was stimulated in the dark

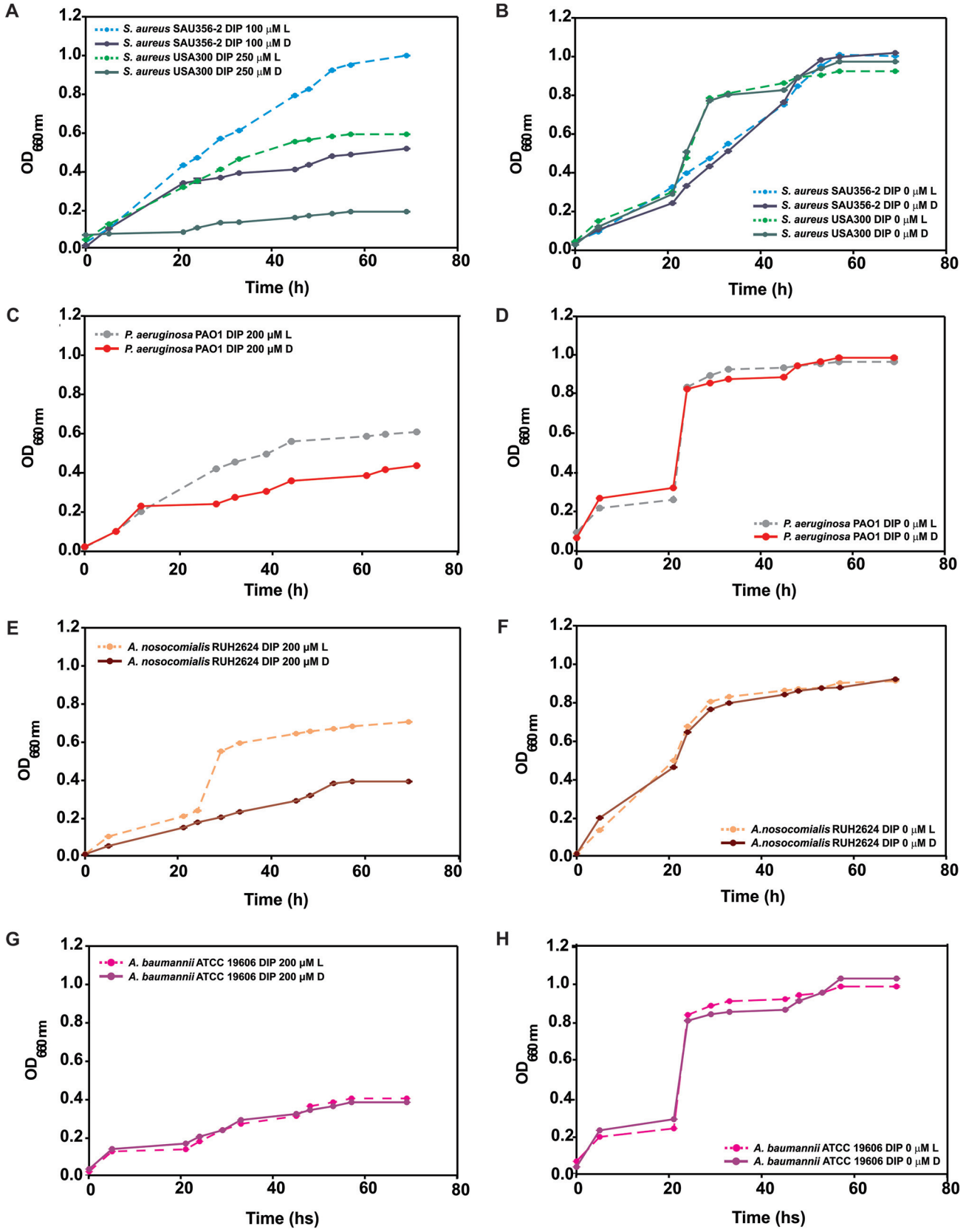

FIG 4 Light modulates growth under iron deprivation in *S. aureus*, *P. aeruginosa*, and *A. nosocomialis* but not in *A. baumannii* at 37°C. (A to D) Growth curves of *S. aureus* SAU356-2 and *S. aureus* USA300 (A) and *P. aeruginosa* PAO1 (C) in TSB medium supplemented with 100, 250, and 200 μM DIP,

(Continued on next page)

compared with illumination conditions (Fig. 5C). Again, no differences were observed in growth, either in the dark or in the presence of light, in minimal media supplemented with acetoin as the sole carbon source in *A. baumannii* ATCC 19606 at 37°C (Fig. 5D). Bacterial growth is not affected by light under our experimental conditions, as similar growth curves were obtained for the different strains in LB broth under blue light and in the dark (Fig. 4F and H). Overall, our results show that light modulates PAA and acetoin catabolism in *A. nosocomialis* but not in *A. baumannii* at 37°C. *S. aureus* USA300 and *P. aeruginosa* PAO1 were not assayed, as they do not grow in M9 medium supplemented with PAA or acetoin as the sole carbon source (not shown).

Modulation of carbohydrate metabolism can also be relevant for bacterial pathogenesis (32). The sugar trehalose has been shown to be involved in colonization and pathogenesis in phytopathogens (33–35). Most bacteria use this disaccharide as a general osmo- and thermoprotectant (36). In addition, mycobacteria produce trehalose-containing glycolipids, which are considered virulence factors (36). Finally, trehalose has been shown to be involved in resistance to desiccation (37) by preserving membranes and labile proteins generating a glassy state (38, 39). Phenotype microarray (Biolog) screenings using the PM1 panel (carbon sources) provided the clue that trehalose catabolism might be modulated by light in *S. aureus* USA300 at 37°C (Fig. S3B). To confirm phenotype microarray results, we performed growth curves of *S. aureus* USA300 in M9 minimal media supplemented with trehalose as the sole carbon source at 37°C. Our results show that growth on 5 mM trehalose as the sole carbon source is supported in the dark, while it is severely inhibited in the presence of light (Fig. 5E). Consistent results were obtained using 10 and 15 mM trehalose (Fig. S3C and D, respectively). The viability of the bacteria was not affected by light, as similar growth curves were obtained for *S. aureus* USA300 in TSB broth under blue light and in the dark (Fig. S3E). Thus, trehalose metabolism is modulated by light in *S. aureus* at 37°C. However, trehalose catabolism was not influenced by light in *A. nosocomialis* RUH2624 (Fig. 5F) or in *P. aeruginosa* PAO1 or ATCC 19606, either at 5 mM or at 10 mM or 15 mM trehalose (not shown).

Light modulates resistance to desiccation in *S. aureus* and *A. nosocomialis*. Resistance to desiccation has been shown to contribute directly to long-term survival, which is key in the ability of *S. aureus* and *Acinetobacter* spp. to spread in the hospital environment and between patients (40–42). So, we next evaluated the effect of light on the ability of *S. aureus* and *A. nosocomialis* to resist desiccation, by inoculating the bacteria on filter papers and determining the viable number at different time points at 37°C. Our results show that *S. aureus* USA300 exhibits higher levels of resistance to desiccation in the dark than under illumination conditions (Fig. 6A). In fact, an abrupt decrease in the number of *S. aureus* USA300 cells is observed during the first 2 days in the dark, remaining relatively constant since then until day 8. On the contrary, the number of viable bacteria under blue light decreased sharply from the beginning, falling below the limit of detection from day 5 onward (Fig. 6A). The *A. nosocomialis* RUH2624 strain showed a similar behavior as *S. aureus* USA300, but interestingly, the differential response to light was maintained much longer in time (Fig. 6B). Our results show that there is approximately a two-order-of-magnitude decrease in the number of bacteria during the first 5 days in the dark, and then it remains relatively constant at least until day 30 (Fig. 6B). But the number of viable bacteria decreased drastically in the presence of light, falling below the limit of detection as early as day 5 and until day 30 (Fig. 6B). Thus, the overall results indicate that light modulates resistance to desicca-

FIG 4 Legend (Continued)
respectively, and control curves in TSB-0 μM DIP (B and D) were incubated stagnantly at 37°C under blue light (L) or in the dark (D). (E to H) Growth curves of *A. nosocomialis* strain RUH2624 (E) and *A. baumannii* strain ATCC 19606 (G) in LB medium supplemented with 200 μM DIP and control curves in LB medium-0 μM DIP (F and H), all incubated stagnantly at 37°C under blue light (L) or in the dark (D). Growth was measured by determining the optical density at 660 nm. Shown is a representative result from three independent experiments. In each experiment, three technical replicates for each strain and condition were included, and error bars indicate the standard deviation of the mean. In some cases, error bars are hidden by the point marker.

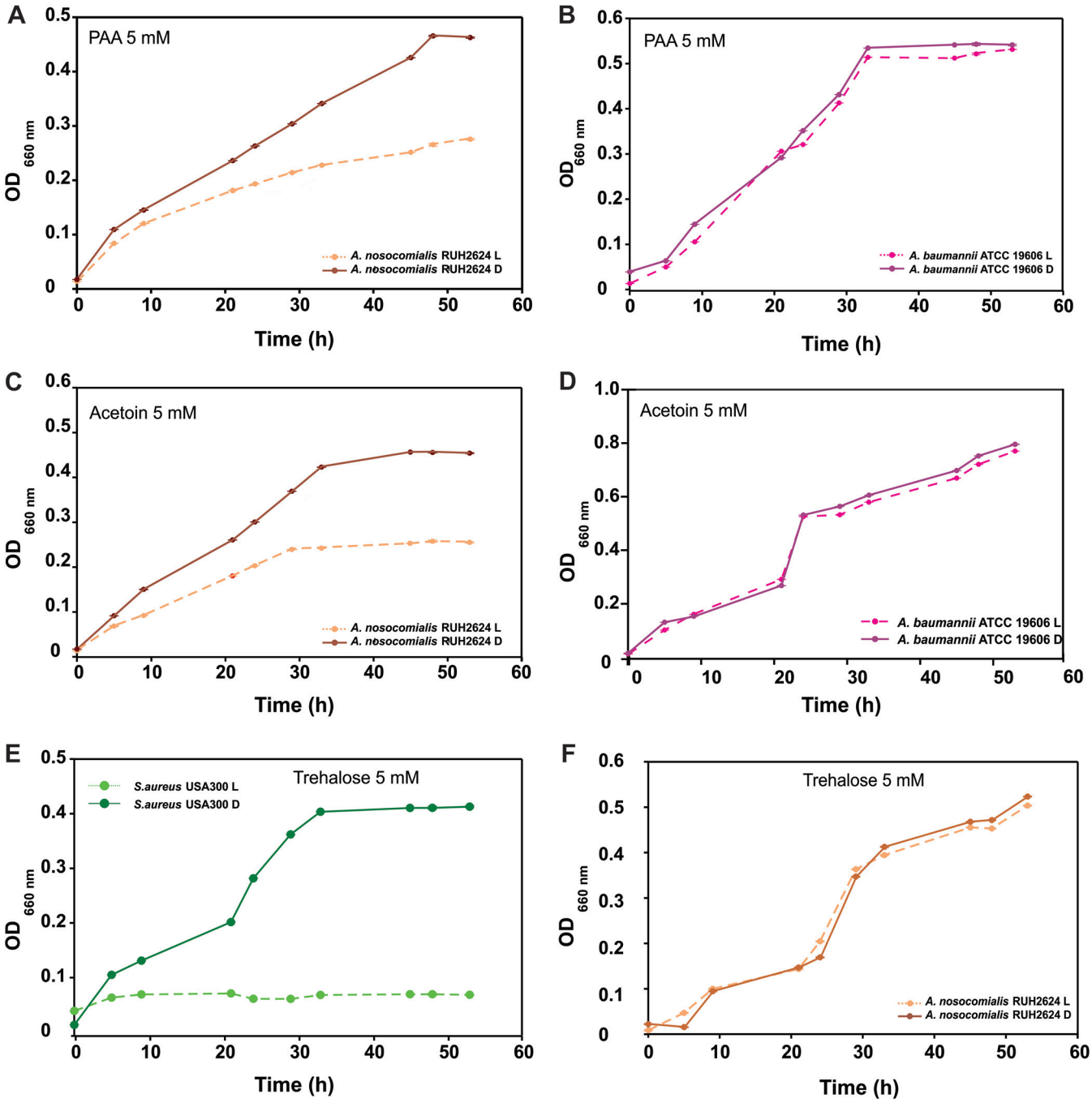

FIG 5 Light modulates PAA, acetoin, and trehalose metabolisms in the pathogens studied. (A to D) Growth curves of *A. nosocomialis* RUH2624 (A and C) or *A. baumannii* ATCC 19606 (B and D) in M9 liquid minimal medium supplemented with 5 mM PAA (A and B) or 5 mM acetoin (C and D) as the sole carbon source, incubated stagnantly at 37°C under blue light (L) or in the dark (D). (E and F) Growth curves of *S. aureus* USA300 (E) or *A. nosocomialis* RUH2624 (F) in M9 liquid minimal medium supplemented with 5 mM trehalose as the sole carbon source incubated stagnantly at 37°C under blue light (L) or in the dark (D). Shown is a representative result from three independent experiments. In each experiment, three technical replicates for each strain and condition were included, and error bars indicate the standard deviation of the mean. In some cases, error bars are hidden by the point marker.

tion in *S. aureus* and *A. nosocomialis* at 37°C, which are relevant findings in the context of the clinical setting.

Light modulates *S. aureus* and *P. aeruginosa* virulence in an epithelial infection model at 37°C. As we have shown above, light modulates very important pathogenesis determinants in *S. aureus*, such as hemolysis, motility, growth under iron limitation, and metabolism. We next evaluated the effect of light on *S. aureus* virulence in an epithelial infection model using a keratinocyte cell line designated HaCaT (43). This model

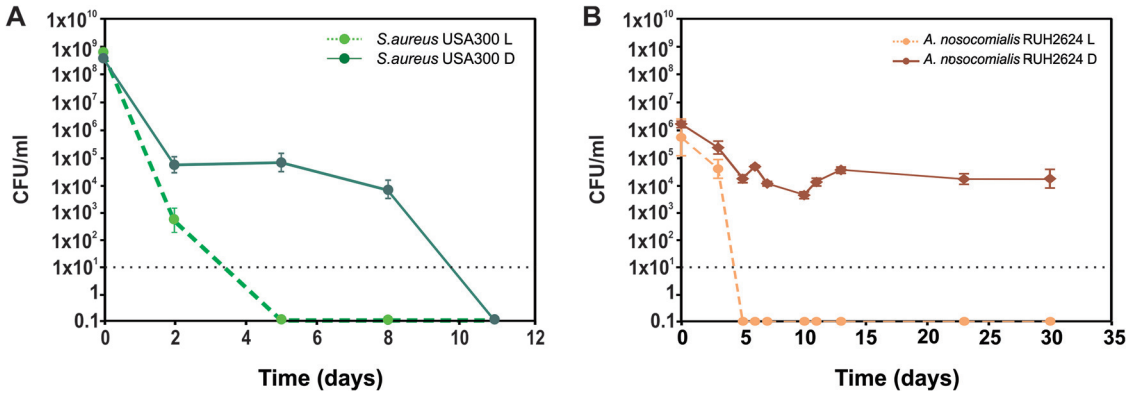

FIG 6 Light modulates resistance to desiccation in *S. aureus* and *A. nosocomialis*. Dried cells located on filter paper pieces were incubated at 37°C under blue light (L) or in the dark (D). Survival was assessed by determining the CFU counts per milliliter at the indicated times points. The data presented are the means from two and three independent experiments in the cases of *S. aureus* and *A. nosocomialis*, respectively, and error bars show the standard error of the mean. Dotted lines represent the limit of detection, which corresponds to 10 CFU/ml in these experiments. All determinations below the limit of detection line received the arbitrary value of 0.1, for plotting purposes.

was chosen since this microorganism is an important skin and soft tissue infection producer (7), and the skin is exposed to light, making it a relevant and useful model to study the effect of light on *S. aureus* skin infections. HaCaT is a nontransformed continuous keratinocyte line of human origin, widely used to study epithelial infection (44, 45), biofilm formation (46), cytotoxicity (47), and skin cancer (48). It is also compatible with skin wound infection models, in which the stratum corneum is disrupted and the bacteria get in direct contact with the living keratinocytes (46). *S. aureus* has been shown to replicate intracellularly in HaCaT cells (49, 50), and therefore, invasion assays were performed. Briefly, HaCaT cells were infected with the bacteria at a multiplicity of infection (MOI) of 100 for 60 min at 37°C. HaCaT cells were then washed and treated with 100 μg/ml gentamicin for 90 min in order to eliminate nonadhered and noninternalized bacteria. Cells were washed again and the medium was replaced as described in the Materials and Methods. Immediately after the infections, the plates were exposed to blue light or kept in the dark for the rest of the experiment. Our results show that at 6 and 24 hours postinfection (PI) with *S. aureus* USA300, a marked reduction in HaCaT survival of approximately 46% and 50%, respectively, was observed when the plates were incubated in the presence of blue light compared with dark conditions (Fig. 7A).

As *P. aeruginosa* is also a clinically relevant pathogen producing skin and soft tissue infections (3) and has also been shown to internalize and replicate in epithelial cells (51, 52), we wondered whether it behaved similarly to *S. aureus* in response to light when facing invasion assays in a HaCaT infection model. In this case, we used an extensively characterized strain, PAO1 (53), as well as the clinical isolate PAE4840 (Table S1). At very short times, such as 2 or 6 h PI with PAO1, no significant differences were detected in HaCaT survival between blue light and darkness (Fig. 7B). On the contrary, at 24 hours PI, a drastic reduction of HACAT survival of approximately 56% for PAO1 and 58% for PAE4840 (Fig. 7B and C, respectively) was observed in the dark compared with light conditions in HaCaT infections.

Controls performed using noninfected HaCaT cells incubated under blue light or in the dark showed that keratinocyte survival was similar between both conditions at each time point assayed (Fig. 7A to C), indicating that light does not affect HaCaT survival. These controls were included in all infection assays performed this work, and similar results were obtained. Moreover, light does not affect bacterial viability, as no differences were detected in growth curves, either for *S. aureus* USA300 grown in TSB medium at 37°C or for *P. aeruginosa* PAO1 or PAE4840 grown in TSB glucose medium at 37°C, in the presence or absence of light (see Fig. S5A to C, respectively, in the supplemental material).

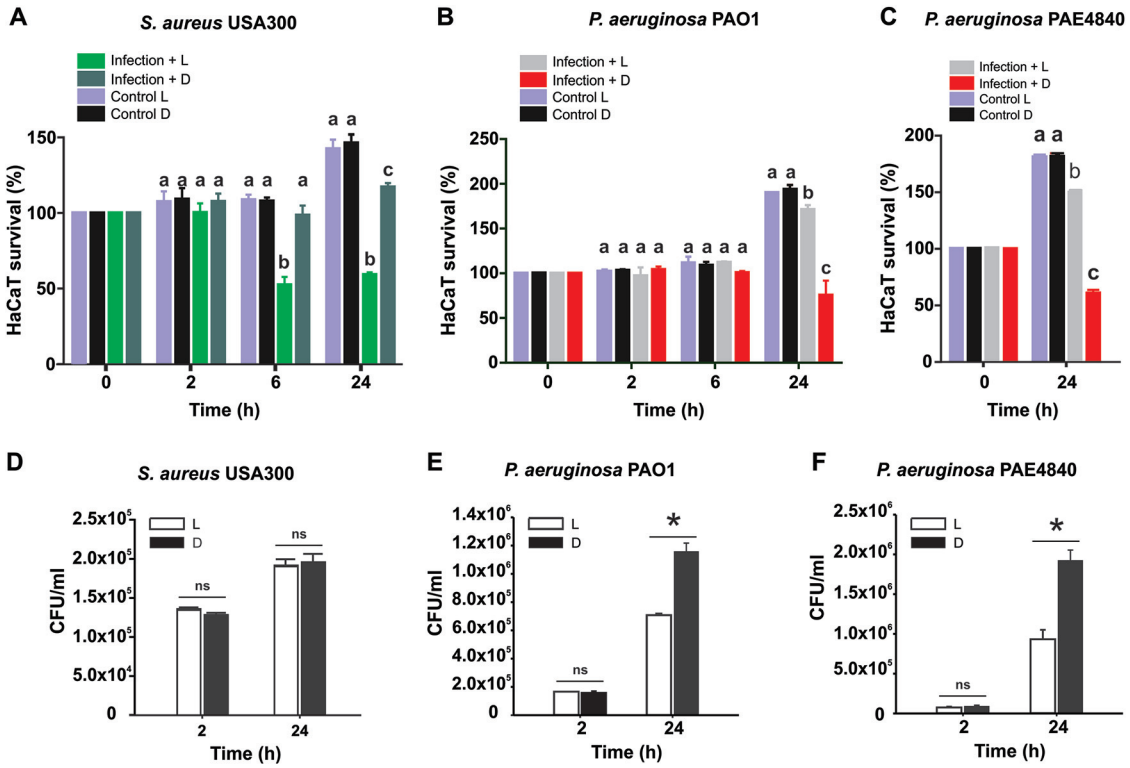

FIG 7 Light modulates virulence of *S. aureus* and *P. aeruginosa* in an epithelial infection model. (A to C) HaCaT cells were infected with the intracellular bacterial pathogens *S. aureus* strain USA300 (A), *P. aeruginosa* strain PAO1 (B), or the clinical isolate PAE4840 (C), and invasion assays were performed as described in Materials and Methods using an MOI of 100. Noninfected HaCaT cell controls, treated with blue light or kept in the dark, are shown for each condition and time point studied. The percent HaCaT survival represents the number of viable HaCaT cells at each light (L) or dark (D) condition and time point assayed, normalized to the number of cells in the uninfected control at time zero, determined by the trypan blue exclusion method. The data are the means and standard deviations of three replicate assays. The mean of the number of cells at time zero was considered 100%. Different letters indicate significant differences as determined by ANOVA, followed by Tukey's multiple-comparison test ($P < 0.05$). These tests were performed comparing data within each time point assayed. The results shown are representative of three independent experiments. (D to F) Bacterial quantification in infected HaCaT keratinocytes. *S. aureus* strain USA300 (D), *P. aeruginosa* strain PAO1 (E), and *P. aeruginosa* PAE4840 clinical isolate (F) were recovered from infected HACAT cells and counted. After invasion assays, keratinocytes were lysed with 0.1% Triton X-100, and the bacteria were recovered and quantified after plating a dilution series onto TSB agar, at 2 and 24 hours postinfection for each light (L) or dark (D) condition, and the plates were incubated at 37°C in the dark. The data represent the means and standard deviations from three replicate assays. Asterisks indicate significant differences between light and dark treatments, as determined by *t* test ($P < 0.05$) performed by comparing data within each time point assayed. ns, not significant. The results shown are representative of three independent experiments.

The results thus far indicate that the application of light resulted in a significant increase in keratinocyte killing by *S. aureus* at temperatures found in warm-blooded hosts, suggesting that light enhances virulence in this microorganism. On the contrary, the application of light resulted in a marked reduction in keratinocyte killing in infections caused by *P. aeruginosa* compared with that of dark conditions at 37°C, showing only a slight decrease compared with noninfected controls both for PAO1 and PAE4840 (approximately 12% and 20%, respectively) (Fig. 7B and C).

The number of *S. aureus* USA300 bacteria recovered from infected keratinocytes was similar under light and dark conditions either at 2 or at 24 hours PI (Fig. 7D), indicating that light does not modulate bacterial internalization and/or replication inside HaCaT cells. In the case of *P. aeruginosa* infections, more bacterial cells were counted in the dark than in the light at 24 h both for PAO1 and PAE4840 (Fig. 7E and F, respectively), suggesting that light modulates the ability of *P. aeruginosa* to replicate intracellularly. This response to light is opposite the effect of light on infected HaCaT survival, which prompted us to hypothesize that light inhibits bacterial replication inside the HaCaT cells leading to reduced HaCaT killing under this condition.

Overall, the response to light was differential in both intracellular pathogens *P.*

aeruginosa and *S. aureus*; virulence was enhanced in the presence of light in *S. aureus*, while in the dark in *P. aeruginosa*.

Light modulates *A. nosocomialis* and *A. baumannii* virulence in an epithelial infection model at 37°C. We next evaluated the effect of light on *A. nosocomialis* and *A. baumannii* virulence using the HaCaT keratinocyte infection model (43), as these microorganisms are also skin infection producers. For this purpose, we first optimized the HaCaT infections with *A. nosocomialis* RUH2624 and determined that this pathogen does not internalize significantly. Thus, we decided to perform adhesion assays (see the supplemental text and Fig. S6). Briefly, *A. nosocomialis* RUH2624 was grown stagnantly for 48 hours in the presence or absence of light, and then the bacteria were added to the monolayers of keratinocytes at an MOI of 100 and incubated for 60 min at 37°C. Immediately after the infection, the unattached bacteria were washed off, and the plates were exposed to blue light or kept in the dark for the rest of the experiment. At 6 hours PI, no significant differences were observed on HaCaT viability under blue light or in the dark (Fig. 8A). However, at 12, 18, and 24 hours PI, we observed decreases of approximately 20%, 31%, and 63%, respectively, in HaCaT survival in the dark compared with illumination conditions (Fig. 8A).

For *A. baumannii* infections, the bacterial cultures were also grown stagnantly, and dark/light conditions were kept during the entire interval of the assay. At early time points, such as 6 and 12 hours PI, no significant differences in the percentage of HaCaT survival was detected between light and dark conditions (Fig. 8B). However, the presence of light generated 32% and 40% increases in keratinocyte killing at 18 and 24 hours PI, respectively, compared with that under darkness conditions (Fig. 8B).

Controls performed using noninfected HaCaT cells showed that light does not affect HaCaT survival (Fig. 8A and B). Moreover, light does not affect bacterial viability, as no differences were detected in growth curves when *A. nosocomialis* RUH2624 or *A. baumannii* ATCC 19606 were grown in LB medium at 37°C stagnantly in the presence or absence of light (Fig. S5D and Fig. 4H, respectively).

HaCaT viability was assayed not only by the trypan blue exclusion method but also by the 3-(4,5-dimethyl-2-thiazolyl)-2,5-diphenyl-2H-tetrazolium bromide (MTT) assay in the cases of *A. nosocomialis* RUH2624 and *A. baumannii* ATCC 19606 (see Fig. S7A to C in the supplemental material), as these microorganisms were used to optimize the virulence assays. MTT results were consistent with the trypan blue exclusion method (Fig. S7A to C), thus validating these assays. Also, the effect of preconditioned medium (PCM) addition instead of Dulbecco's modified Eagle's medium (DMEM) was assayed in the case of *A. nosocomialis* RUH2624 infections (see the supplemental material). It should be noted that PCM has been shown to be required by different pathogens to kill *C. albicans* (54), and thus, we evaluated its effect in the HaCaT infection model. However, a similar tendency as DMEM was observed in HaCaT survival between blue light and dark conditions (Fig. S7D and E).

Overall, the data obtained here indicate that light reduces *A. nosocomialis* virulence against a HaCaT infection model at temperatures found in warm-blooded hosts (Fig. 8A). In *A. baumannii*, light also shows an important effect on virulence modulation, which in this case is opposite to that observed for *A. nosocomialis* (Fig. 8B). The differences observed in the virulence of these microorganisms between light or dark in the adhesion assays were not due to a differential adhesion or replication during the infection, as determined by bacterial enumeration at 2 and 24 h PI (Fig. 8C and D).

The photoreceptor BlsA and the T6SS are not involved in modulation by light of *A. baumannii* virulence in an epithelial infection model at 37°C. Previous studies have shown that the type VI secretion system (T6SS) of several Gram-negative pathogens is involved in competition with other microorganism for the colonization of different niches (55). Also, its presence has been related to resistance to human serum and a more active formation of biofilms (56). However, less evidence has been gathered regarding the role of T6SS in *A. baumannii* virulence in eukaryotic hosts. On the other hand, the photoreceptor BlsA has been described as a global regulator modulating different aspects related to bacterial persistence, virulence, and antibiotic susceptibility

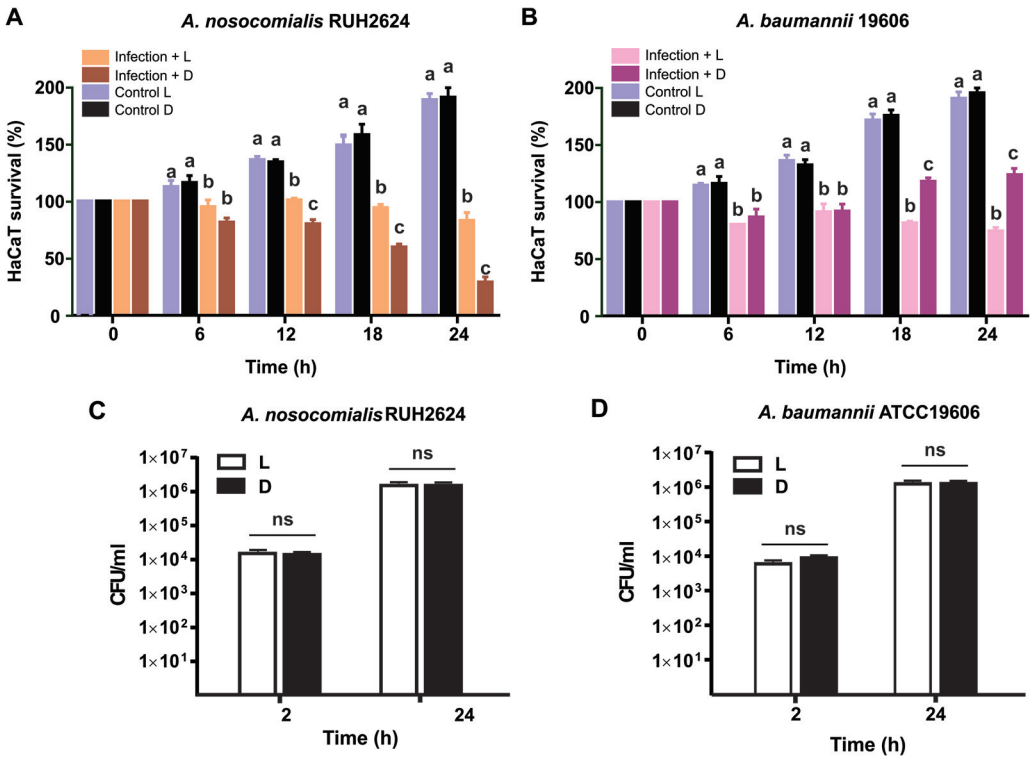

FIG 8 Light modulates virulence of *A. nosocomialis* and *A. baumannii* in an epithelial infection model. (A and B) HaCaT cells were infected with the noninternalizing bacterial pathogens *A. nosocomialis* RUH2624 (A) and *A. baumannii* ATCC 19606 (B), and adhesion assays were performed as described in Materials and Methods, with an MOI of 100 in each case. Noninfected HaCaT cell controls, treated with blue light or kept in the dark, are shown for each condition and time point studied. The percent HaCaT survival represents the number of viable HaCaT cells at each light (L) or dark (D) condition and time point assayed, normalized to the number of cells in the uninfected control at time zero, determined by the trypan blue exclusion method. The data are the means and standard deviations of three replicate assays. The mean number of cells at time zero was considered 100%. Different letters indicate significant differences as determined by ANOVA, followed by Tukey's multiple-comparison test ($P < 0.05$). These tests were performed by comparing data within each time point assayed. The results shown are representative of three independent experiments. (C and D) Bacterial quantification in infected HaCaT keratinocytes. *A. nosocomialis* strain RUH2624 (C) and *A. baumannii* strain ATCC 19606 (D) were recovered from infected HACAT cells and counted. After adhesion assays, keratinocytes were lysed with 0.1% Triton X-100, and the bacteria were recovered and quantified after plating a dilution series onto LB agar plates, at 2 and 24 hours postinfection for each light (L) or dark (D) condition, and the plates were incubated at 37°C in the dark. The data represent the means and standard deviations of three replicate assays. The data were analyzed by *t* test performed by comparing data within each time point assayed, and no significant differences (ns, not significant) were found ($P < 0.05$). The results shown are representative of three independent experiments.

in *A. baumannii* at environmental temperatures (10–18). In order to analyze the involvement of T6SS and BlsA on the effect of light in *A. baumannii* virulence against the HaCaT infection model, we carried out similar adhesion assays as above using two isogenic mutants, namely, Δ*tssM* and Δ*blsA* (10). TssM forms, in combination with other proteins, the membrane complex upon which the macromolecular syringe of the T6SS is assembled. Thus, a *tssM* mutant would be defective in the production of an essential component required for T6SS functioning (57). As shown previously, *A. baumannii* ATCC 19606 virulence was significantly modulated by light, with enhanced HaCaT killing of approximately 32% and 23% at 18 and 24 h, respectively, under blue light compared with under darkness (Fig. 9A). However, neither Δ*tssM* nor Δ*blsA* mutants showed significant differences in keratinocyte survival compared with the wild-type between blue light and dark conditions in adhesion assays in the HaCaT infection model (Fig. 9A). Controls performed using noninfected HaCaT cells show that light does not affect HaCaT survival (Fig. 9B). Thus, the overall evidence indicates that neither TssM nor the photoreceptor BlsA is involved in the response to light of the pathogen's virulence under the tested conditions.

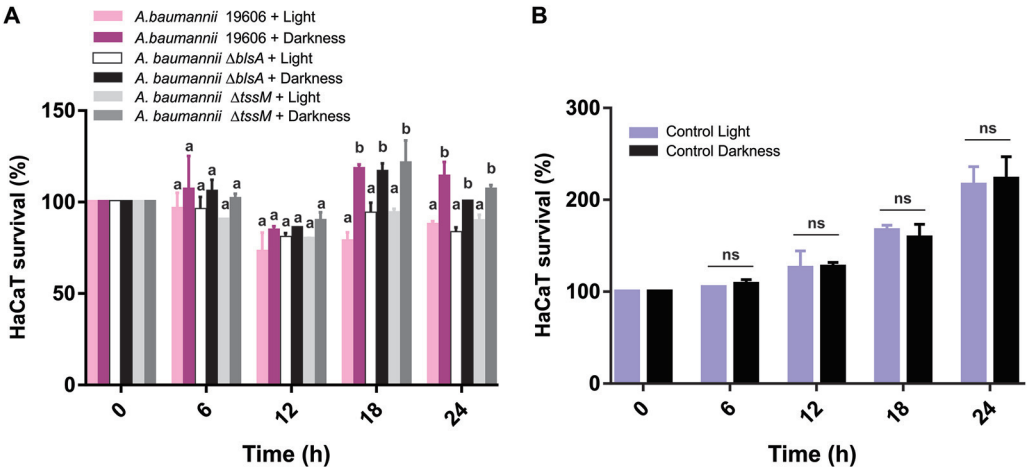

FIG 9 BlsA and TssM do not contribute to photoregulation of virulence of *A. baumannii* against a HaCaT model. (A) HaCaT keratinocytes were infected with *A. baumannii* ATCC 19606 and derived strains Δ*blsA* and Δ*tssM*, and adhesion assays were performed as described in Materials and Methods using an MOI of 100. (B) Noninfected HaCaT controls, treated with blue light or kept in the dark, are shown for each condition and time point studied. The percent HaCaT survival represents the number of viable HaCaT cells at each light (L) or dark (D) condition and time point assayed, normalized to the number of cells in the uninfected control at time zero, determined by the trypan blue exclusion method. The data are the means and standard deviations from three replicate assays. The mean number of cells at time zero was considered 100%. In A, different letters indicate significant differences, as determined by ANOVA, followed by Tukey's multiple-comparison test ($P < 0.05$). These tests were performed by comparing data within each time point assayed. The data in panel B were analyzed by *t* test performed by comparing data within each time point assayed, and no significant differences (ns, not significant) were found ($P < 0.05$). The results shown are representative of three independent experiments.

Coinfection with *A. baumannii* and *A. nosocomialis* alters the light-modulated virulence pattern against an epithelial infection model. Considering that *A. baumannii* and *A. nosocomialis* showed opposite behaviors during adhesion assays in response to illumination, we decided to analyze the effect of light on the outcome of a coinfection produced by both species, as polymicrobial infections are common in patients (58, 59). To this end, we coinfected HaCaT keratinocytes with *A. baumannii* ATCC 19606 and *A. nosocomialis* RUH2624 at a 50/50 ratio and at an MOI of 100 or 30. When an MOI of 100 was used, no significant differences were quantified at 2 h PI between the coinfection and the controls, either under light or under dark conditions (Fig. 10). At 6 h PI, a small but significant decrease in the percentage of HaCaT survival was detected for the coinfection compared with the uninfected controls, but no differences were detected between light and dark conditions (Fig. 10). Unexpectedly, at 24 h PI, a strong reduction of HaCaT survival was observed for the coinfection in the presence of light, with practically no cells recovered; while 20% of HACAT cells were still counted in the dark (Fig. 10). Thus, coinfection with both pathogens, *A. baumannii* and *A. nosocomialis*, at an MOI of 100 resulted in a pattern that resembles that of *A. baumannii*, i.e., more virulent in the presence of light. Using an MOI of 30, no modulation by light was observed, and HaCaT killing was, as expected, not as drastic (see Fig. S8 in the supplemental material). No significant differences were obtained in coinfection assays, either in the total number of adherent bacteria (CFU per milliliter) recovered from HaCaT cells under blue light or dark conditions or for *A. baumannii*, which was determined by plating in LB containing ampicillin, or for *A. nosocomialis*, which was calculated by subtracting the two values, at 2 and 24 h PI and MOI of 100 or 30 (not shown).

Light modulates the ability of *A. nosocomialis* and *A. baumannii* to kill *C. albicans* at 37°C. Given the results shown above regarding the significant effect of light on bacterial virulence in the HaCaT infection model at temperatures found in warm-blooded animals, as well as the differential response to light between *A. nosocomialis* and *A. baumannii*, we intended to evaluate the effect of light on the ability of these bacteria to kill competitors, such as *C. albicans* at 37°C. *C. albicans* is a microorganism potentially sharing habitat with *A. baumannii* in the clinical setting (10) and has been shown

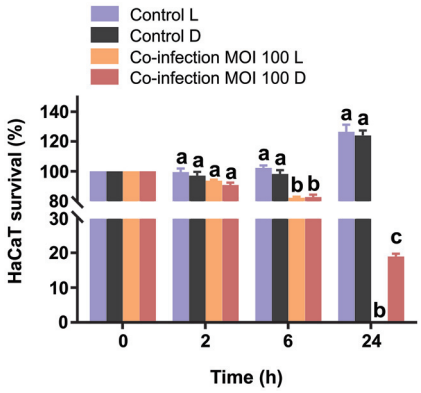

FIG 10 Effect of light on the outcome of a coinfection by *A. baumannii* ATCC 19606 and *A. nosocomialis* RUH2624 against an epithelial infection model. HaCaT cells were infected with an MOI of 100 (50 each bacterium), and adhesion assays were performed as described in Materials and Methods. Noninfected HaCaT cells controls, treated with blue light or kept in the dark, are shown for each condition and time point studied. The percent HaCaT survival represents the number of viable HaCaT cells at each light (L) or dark (D) condition and time point assayed, normalized to the number of cells in the uninfected control at time zero, determined by the trypan blue exclusion method. The data are the means and standard deviations from three replicate assays. The mean number of cells at time zero was considered 100%. Different letters indicate significant differences, as determined by ANOVA, followed by Tukey's multiple-comparison test ($P < 0.05$). These tests were performed by comparing data within each time point assayed. The results shown are representative of three independent experiments.

to cause polymicrobial infections with the aforementioned pathogens (59). For killing assays, *C. albicans tup1* mutants were used, as it was previously shown that *A. baumannii* cells are able to attach to and kill *tup1* filaments but not the parental SC5314 yeast cells (54). Coincubation of *tup1* mutant filaments with *A. nosocomialis* RUH2624 cells resulted in a time-dependent increase of fungal death under blue light at 37°C, while killing was drastic in the dark with null or negligible fungal CFU registered from 24 hours onward (Fig. 11A). Controls performed by incubating fungal filaments in sterile medium or PCM in the presence of blue light and in the dark at 37°C show that there is no effect of light on *C. albicans* killing under the conditions used (Fig. 11B). Thus, as occurred with the HaCaT virulence model, light reduces the ability of *A. nosocomialis* to kill *C. albicans* at 37°C.

Coincubation of *tup1* mutant filaments with *A. baumannii* ATCC 19606 cells also resulted in a time-dependent increase of fungal death at 37°C, which was more drastically pronounced in the presence of light than in darkness (Fig. 11C). In fact, differences in *C. albicans* survival between light and dark conditions were observed as early as 4 hours and were amplified drastically from 24 hours onward, the time point from which the amount of recovered *C. albicans* fell below the limits of detection (Fig. 11C). Controls show no effect of light on *C. albicans* viability under the conditions used (Fig. 11D). Thus, as occurred with the HaCaT virulence model, light stimulates the ability of *A. baumannii* to kill *C. albicans* at 37°C. The *A. baumannii* ATCC 19606 Δ*blsA* mutant behaved in a similar fashion as the wild type, without showing statistically significant differences between light and dark at any of the time points analyzed (Fig. 11D), suggesting that BlsA is not involved in the light response at this temperature.

DISCUSSION

In this work, we show that light modulates important pathogenicity determinants and virulence in priority pathogens, such as *S. aureus*, *P. aeruginosa*, *A. baumannii*, and *A. nosocomialis*, at temperatures found in warm-blooded hosts. Our results show that light modulates hemolysis, motility, growth under iron-deprivation conditions, metabolism, resistance to desiccation, and virulence at 37°C, depending on the particular pathogen. In *S. aureus*, we have found that light modulates hemolysis, which was

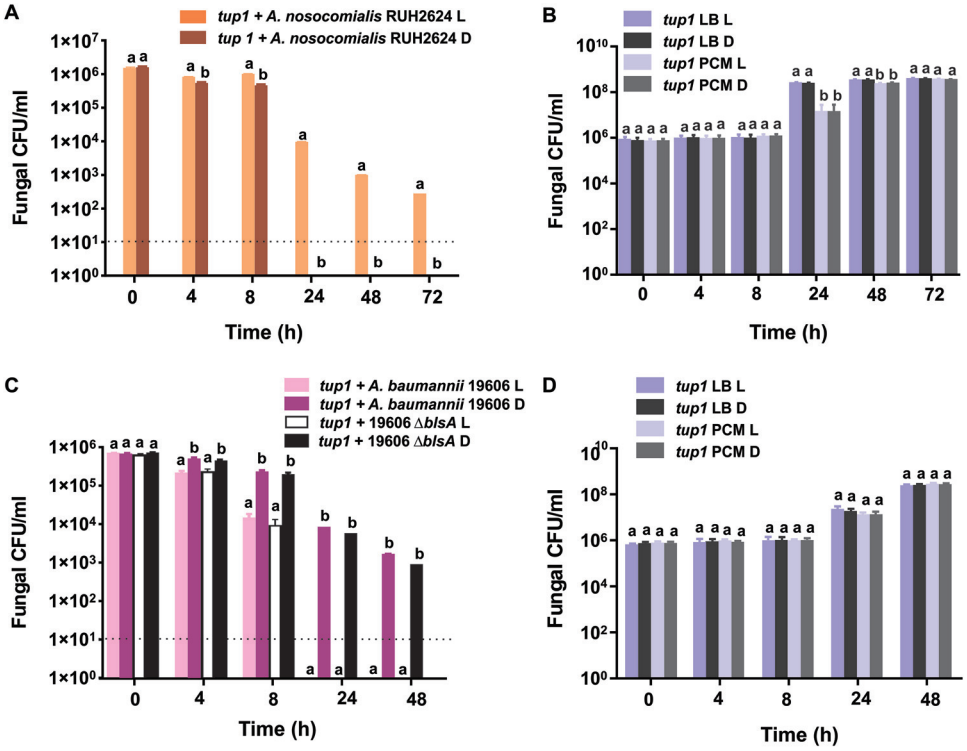

FIG 11 Effect of light on killing of the *C. albicans tup1* mutant by *A. nosocomialis* and *A. baumannii* cells. (A) Fungal filaments were incubated in medium inoculated with *A. nosocomialis* RUH2624 cells either in the presence of blue light (L) or in darkness (D). (B) Fungal filaments were incubated in sterile LB medium or sterile PCM medium either in the presence of blue light (L) or in darkness (D), as controls. (C) Fungal filaments were incubated in medium inoculated with *A. baumannii* ATCC 19606 or derived strains such as the isogenic mutant Δ*blsA* either in the presence of blue light (L) or in darkness (D). (D) Fungal filaments were incubated in sterile LB medium or sterile PCM medium either in the presence of blue light (L) or in darkness (D), as controls. Dotted lines represent the limit of detection, which corresponds to 10 CFU/ml in these experiments. All determinations below the limit of detection line received the arbitrary value of 0.1, for plotting purposes. The data are the means and standard deviations of three replicate assays. Different letters indicate significant differences, as determined by ANOVA, followed by Tukey's multiple-comparison test ($P < 0.05$). These tests were performed by comparing data within each time point assayed. The results shown are representative of three experiments.

enhanced in the dark and limited in the presence of light. This activity depends on the alpha-toxin, as hemolysis is lost in the *hla* mutant and photoregulation of hemolysis is restored in the complemented strain. *S. aureus* can express a variety of resistance mechanisms and virulence factors, allowing it to evade host natural defenses. Among them, toxins such as alpha-toxin are able to degrade some of the host cells, manipulate the innate and adaptive immune responses, and degrade intercellular junctions (22). This has an obvious contribution in *S. aureus* proliferation and disease (7). In fact, the identification of α-hemolysin receptors has highlighted the key role of this virulence factor in several *S. aureus* diseases involving epithelial barrier disruption (22). Staphylococcal invasion of human keratinocytes, which leads to necrotic and apoptotic cell damage, represents a potent trait contributing to bacterial pathogenesis (49).

Iron is a ubiquitous component of all living cells, with only a few exceptions (29). For a microorganism to develop its pathogenic potential and be able to grow and multiply within the body, it must obtain iron from the host (29). We have recently shown that light modulates iron uptake through the BlsA photoreceptor in *A. baumannii* at environmental temperatures, resulting in a much poorer capability to grow under blue light than in the dark at 23°C (15). Insights into the mechanisms showed that BlsA interacts with and antagonizes the functioning of the Fur repressor, resulting in modulation by light of the acinetobactin siderophore expression at environmental

temperatures (15). Results presented here show that *S. aureus*, *P. aeruginosa*, and *A. nosocomialis* are more efficient at circumventing iron deficiency in the presence of blue light than in the dark at 37°C. The enhanced production of siderophores, in analogy to what happens in *A. baumannii* (15), might be taking place in the presence of light. Hemolysis, which releases heme from hepatocytes, the preferred iron source of *S. aureus* (60), is enhanced in the dark rather than under blue light. It is thus apparent that *S. aureus* counts with diverse mechanisms to obtain iron under blue light and dark conditions. However, further investigation will be required to determine which system is required at each particular situation along *S. aureus*' pathogenic life in response to illumination.

Comparable to *A. baumannii* at 23°C, *A. nosocomialis* also shows repression of PAA catabolism in the presence of light at 37°C, a metabolism previously shown to be involved in *A. baumannii* virulence (23). Furthermore, we show that light also modulates trehalose metabolism in *S. aureus*, a disaccharide known to be involved in resistance to desiccation, osmo- and thermoprotection, and virulence (37–39), as well as resistance to desiccation in *S. aureus* and in *A. nosocomialis*. The capacity of pathogenic microorganisms to persist in an intrahospital environment is considered a key aspect in their marked success as pathogens, as it favors the spread of multidrug-resistant clones causing nosocomial infections and outbreaks (61).

Most interestingly, using an epithelial infection model, we demonstrated that light has an effect on the virulence of these pathogens. Given that these microorganisms are responsible for severe skin infections and that the skin is a light-exposed tissue, the choice of keratinocytes as the infection model appears to be pertinent. Alternative therapies for treatment of these pathogens are urgently needed, and the use of new options, such as antibiotics in combination or with adjuvants, bacteriophages, antimicrobial peptides, nanoparticles, and light therapies are gaining increasing interest (2). According to our results, the direct application of low-intensity blue light reduces the virulence of some pathogens, such as *P. aeruginosa* and *A. nosocomialis*, in epithelial infection models, suggesting that it could be used as a sole or combined tool to control human infections. Light was also found to modulate the outcome of infections caused by *S. aureus* and *A. baumannii*, even though in the opposite way. In these cases, detailed knowledge about the mechanisms governing the response to light would be required to keep the regulatory switch in the lowest virulence/persistence configuration possible. Importantly, the low-intensity blue light and doses applied in this work do not alter keratinocyte viability, measured as the percentage of keratinocyte survival. Nevertheless, the possibility exists that minor changes in host cell gene expression could still be occurring at a less obvious level that could affect the complex host-pathogen interactions. Most developing light therapies designed to control infections are based on the application of high light intensities and doses, often in the presence of photosensitizers, to achieve antimicrobial photoinactivation (photodynamic inactivation [PDI]) (2, 4, 62). The mechanism of action of PDI is not yet well understood, but it is commonly hypothesized that endogenous or exogenously provided photosensitizing chromophores are excited by antimicrobial light, which in turn produces cytotoxic reactive oxygen species (ROS) through a photochemical process (63). Major drawbacks are related to the use of UV light or visible light at high intensities and doses which produce cytotoxic effects that spread to the host cells (63) and compromise their application in patients (2, 4). The mechanism underlying in our experimental setup is completely different; bacterial viability is not compromised but rather regulatory processes in response to light are taking place, which include transcriptional modulation by light of bacterium-specific genetic pathways (10–18), in the presence of very low intensity and doses of blue light (6 to 10 μmol photons/m^2/s). Only a few PDI reports use blue light in the absence of exogenous photosensitizers, such as in the murine skin abrasion infection model reported by Amin et al., in which a blue light intensity of 4,600 μmol photons/m^2/s was applied with a total light exposure up to 240 J/cm^2 to inactivate *P. aeruginosa* (64). Also, in another work reported by Wang et al., a blue light intensity

of 4,600 μmol photons/m^2/s was applied up to a total dose of 360 J/cm^2 to treat *A. baumannii* infection using a mouse burn infection model (63). However, in these works, the effect of light on host tissues was not assessed, and additional studies demonstrating the efficacy and safety of PDI against ESKAPE infections are required (2).

Globally, the use of light allows local treatments (62), is inexpensive, and is accessible, and low-intensity blue light does not damage the uninfected tissue cells (63–65). From the data shown here, it follows that the design of a potential light therapy should take into account the identity and composition of the microorganisms producing the infection. In fact, coinfection studies, in our system, show that *A. baumannii* dominates the virulence scenario over *A. nosocomialis* on an epithelial infection model.

Opposite behaviors have been observed in the response to light between the different ESKAPE pathogens, e.g., the ability to grow under iron-deprived conditions is stimulated in the presence of light for *S. aureus*, *P. aeruginosa*, and *A. nosocomialis* at 37°C, while inhibited in *A. baumannii* at 23°C. Also, acetoin catabolism is repressed by light in *A. nosocomialis* at 37°C, while it is induced in *A. baumannii* at 23°C. Finally, different pathogenic species showed differential virulence responses to light. *A. baumannii* and *S. aureus* increase their virulence in response to light, while *P. aeruginosa* and *A. nosocomialis* decrease it. It is thus evident that the light signal transduction circuits vary among pathogens, leading to different responses to light, which more likely reflects bacterial adaptations to particular niches as well as lifestyles in the environment or as pathogens in a host.

C. albicans is an eukaryotic microorganism sharing ecological niches with *A. baumannii*, and it is widely used as a model to study bacterial virulence (10). Coincubation of *A. baumannii* with *C. albicans* showed a dramatic enhancement of *A. baumannii*-mediated killing of *C. albicans* filaments through the photoreceptor BlsA in the presence of blue light at 23°C (10). In this work, we further show that light enhances the ability of *A. baumannii* to kill *C. albicans* at 37°C, through a BlsA-independent mechanism. It is not surprising that BlsA is not involved in the ability of *A. baumannii* to kill *C. albicans* at 37°C since we have previously shown that this photoreceptor is functional only at environmental temperatures (10, 17, 18). These results add strong evidence on the presence of another noncanonical photoreceptor still to be identified in *A. baumannii*, which has been already proposed (14). Interestingly, modulation of virulence by light followed similar patterns in *A. baumannii* and *A. nosocomialis* both against *C. albicans* or in an epithelial infection model; i.e., light stimulated virulence in *A. baumannii*, while the application of light reduced virulence in *A. nosocomialis* (57).

Work is currently being conducted to identify the photoreceptors involved in light sensing in these pathogens. To our knowledge, *S. aureus* has not been previously shown to sense and respond to light, and no traditional photoreceptors were reported to be encoded in its genome. By sequence analyses, we were able to identify two GAF domain-containing proteins (see Table S2 in the supplemental material), but their function as photoreceptors has not been corroborated yet. In *P. aeruginosa*, the KinB-AlgB-BphP module has been shown to modulate biofilm and virulence genes in response to a far-red light signal at environmental temperatures such as 25°C: Phospho-AlgB represses biofilm and virulence genes, KinB dephosphorylates and thereby inactivates AlgB, while the photoreceptor BphP is the kinase that, in response to light, phosphorylates and activates AlgB (66). The *P. aeruginosa* genome does not encode LOV or BLUF domain proteins but possesses BphP as the only identifiable photoreceptor (see Table S2 in the supplemental material), which in addition to far-red light is also capable of detecting blue and red light as well (66). Also, a RmcA sensory domain predicted to bind a flavin cofactor (Table S2) was suggested to be involved in blue light-dependent inhibition of biofilm wrinkle formation also at environmental temperatures (67). However, further research will be essential to determine whether these photoreceptors are responsible for the response to blue light observed at 37°C in this work. In *A. baumannii*, the BLUF-type BlsA photoreceptor has been shown to function at environmental temperatures (10, 17, 18) (Table S2), and only recently has the presence of putative

KinB-AlgB-BphP homologs been predicted to be encoded in the *A. baumannii* genome (66) (Table S2); however, their functioning has not yet been ascertained. Despite that responses to light independent of BlsA have already been reported in *A. baumannii* (13, 68), the photoreceptor involved in these responses is still to be identified. Finally, *A. nosocomialis* encodes three BLUF-type photoreceptors (19) (Table S2), which are currently under study.

Overall, we provide new fundamental knowledge regarding the physiology of important ESKAPE pathogens, as well as the basis for potential safe light therapies. Our next goal is to assay the combination of light with antimicrobial agents to determine if synergistic effects could be achieved to control infections.

MATERIALS AND METHODS

Bacterial strains. The *S. aureus* clinical isolates used in this study were recovered from either ambulatory or hospitalized patients in a public hospital from Rosario, Argentina, during 2018 (see Table S1 in the supplemental material). Two isolates presented multidrug-resistant (MDR) phenotypes (Table S1). MDR is defined as nonsusceptibility to at least one agent in three or more antimicrobial categories (69). *S. aureus* USA300 is an extensively characterized methicillin-resistant strain whose genome has been sequenced (GenBank accession number CP019590) and is frequently used as model (25). *S. aureus* USA300 *hla* and *hla* isogenic mutants harboring plasmid pAH5 expressing a wild-type copy of *hla* were provided by Jovanka Voyich from Montana State University (26), while *S. aureus* USA300 *agr* and *sae* mutant series were obtained from the Nebraska collection (University of Nebraska Medical Center). *S. aureus* RN4220 is a commonly used laboratory strain with a known defect in *agrA*, which affects the secretion of numerous toxins and thus shows reduced virulence (24). *P. aeruginosa* PAO1 is a spontaneous chloramphenicol-resistant mutant of the original PAO strain that had been isolated in 1954 from a wound in Melbourne, Australia (53). *P. aeruginosa* PAE4840 is a clinical isolate recovered from a peripheral venous catheter from a patient hospitalized in the same public hospital of Rosario mentioned above in July 2019 (Table S1). All clinical isolates recovered from the public hospital from Rosario were phenotypically identified as *S. aureus* (indicated as SAU) or *P. aeruginosa* (indicated as PAE) by the Vitek system (bioMérieux, France). *A. baumannii* 19606 and 17978 strains were obtained from ATCC. *A. baumannii* Ab33405 is an indigo-pigmented strain that belongs to the clonal complex CC113B/CC79P and possess resistance to different antibiotic families (trimethoprim, florfenicol, β-lactam, aminoglycoside, and sulfonamide) (70). *A. nosocomialis* RUH2624 is a clinical isolate recovered from forehead skin (20).

Construction of the *A. baumannii* ATCC 19606 *tssM* isogenic insertion derivative. A 2,062-bp fragment containing a region of the *tssM* gene was PCR amplified using primers tssMEF (5′-GAATTCCAACTTTCCCAAATTGCT-3′) and tssMER (5′-GAATTCCGTTGGAAGTTCATAACA-3′), which harbor EcoRI tails. The amplicon was cloned into the pBluescript SK− plasmid, in which the pUC4K PstI restriction fragment harboring the DNA kanamycin resistance (Kn^r) cassette was inserted into the unique NsiI site located at nucleotide 1000 of the amplified *tssM* fragment to generate pBluescript-*tssM*-Kn. This fragment was subsequently subcloned into the EcoRI sites of pKNOCK-Amp, and the resulting plasmid is pKnock-*tssM*-Kn. *Escherichia coli* EC100D$^+$ cells harboring pKnock-*tssM*-Kn, *E. coli* HB101 cells harboring pRK2073, and *A. baumannii* ATCC 19606 cells were used as donor, helper, and recipient strains, respectively, in triparental conjugations. Transconjugants were selected on Simmons citrate agar plates containing 40 μg/ml Kn. Total DNA was isolated from a putative *A. baumannii* ATCC 19606 *tssM* insertional derivative, which was resistant to Kn and sensitive to 500 μg/ml ampicillin (Amp), and used to confirm the nature of the site-directed insertion mutation by PCR with primers tssMEF and tssMER. The presence of only one copy of the Kn resistance cassette in the *A. baumannii* 19606 *tssM* mutant was verified by reverse transcription-quantitative PCR (qRT-PCR).

Blue light treatments. Blue light treatments were performed as described in our previous studies (10). Briefly, cells were incubated for 24 h (or else as specified) at 37°C in the dark or under blue light emitted by 9 light-emitting diode (LED) arrays, with an intensity of 6 to 10 μmol photons m^{-2} s^{-1}. Each array was built using 3 LED module strips emitting blue light, with emission peaks centered at 462 nm, which were determined using a Lo-Cor LI-1800 spectroradiometer (10).

Hemolysis assays. The different *S. aureus* strains assayed were grown overnight at 37°C in TSB media. A total of 10 μl of cultures grown to an optical density at 660 nm (OD_{660}) of 2.5 were inoculated as spots onto the surface of sheep blood agar commercial plate (Columbia; bioMérieux) pairs. Plates were inspected and photographed after incubation under blue light or in the dark at 37°C for 48 hours or else specified. The area of the zone of clearance was determined as the difference between the area of the hemolytic halo and the area of the bacterial spot, measured with ImageJ (NIH). Three independent experiments were performed.

Real-time reverse transcription-quantitative (qRT-PCR). Bacterial RNA was extracted from *S. aureus* USA300 cells grown under blue light or in the dark on sheep blood agar plates for 48 hours at 37°C using TRIzol reagent (Invitrogen Life Technologies), according to the manufacturer's protocol. RNA was subjected to DNase treatment using a RQ1 RNase-free DNase (Promega). Retrotranscription and qRT-PCR experiments were done as described in Muller et al. Expression of *hla* and *rpoB* genes was assayed using the following primer pairs: *hlaF* (5′-GGCCTTATTGGTGCAAATGT-3′) and *hlaR* (5′-CCATATACCG GGTTCCAAGA-3′) and *rpoBF* (5′-ACAGTATTGTTACGTGCATTAGG-3′) and *rpoBR* (5-CAGTTGGTGGTTCA

CCTGGACG-3′). Relative expression ($-\Delta C_T$) value represents the difference in threshold cycle (C_T) between *hla* and control (*rpoB*) genes.

Cell motility assays. Cell motility was tested on 1% tryptone, 0.5% NaCl, and 0.3% agarose plates inoculated on the surface by depositing 3 μl of tryptic soy broth (TSB) cultures grown to an optical density at 660 nm (OD_{660}) of 0.3. The plates were incubated overnight (24 hours) in the presence or absence of blue light at 37°C. Three independent experiments were performed.

Growth under iron limiting conditions. To test the ability of *S. aureus* USA300, *P. aeruginosa*, *A. baumannii*, and *A. nosocomialis* to grow under iron deprivation conditions, 1/100 dilutions of overnight cultures grown in TSB at 37°C in the case of the first two microorganisms, or in Luria-Bertani (LB) medium (Difco, San Jose, CA) for the last two, were inoculated in the corresponding liquid medium supplemented or not with the indicated iron chelator 2,2′-dipyridyl (DIP) concentrations. Please note that the use of different concentrations of DIP is necessary for the different species, as the microorganisms exhibit differential sensitivity to this agent (MIC). Cultures were subsequently grown stagnantly in 96-well microtiter plates at 37°C under blue light or in the dark. At the time points indicated in the figures, the OD_{660} of the culture was determined using an Epoch 2 microplate spectrophotometer (BioTek). Three independent experiments were performed, with each including three replicates for each strain and condition. No light sensitivity was observed for DIP under the experimental conditions used (see the supplemental text and Fig. S4).

Biolog MicroArrays. Phenotype MicroArrays (Biolog, CA) were used to test the effect of light on the ability of *S. aureus* USA300 to grow using different carbon sources (carbon sources assay panels PM1). Briefly, bacterial cells were cultured in TSB at 37°C for 18 hours. Then, the cells were washed twice with 1× phosphate-buffered saline (PBS) (0.137 M NaCl, 0.0027 M KCl, 0.01 M Na_2HPO_4, and 0.0018 M KH_2PO_4; pH ≈ 7.4; Thermo), and the pellet was resuspended in inoculating fluid (IF-0) buffer (Biolog) adjusting the OD_{660} to 0.35 to 0.4. A 1:5 dilution was prepared in IF-0 plus dye by following the manufacturer's instructions (final OD_{660} of approximately 0.06), and 100 μl of this cell suspension was inoculated in each well of duplicate PM1 plates. The plates were then incubated stagnantly for 24 hours at 37°C under blue light or in the dark, and results were read at A_{590} using a Synergy 2 multimode plate reader (BioTek, USA) and Gen5 microplate reader software (BioTek).

Growth on different carbon sources. To test the ability of *S. aureus*, *P. aeruginosa*, *A. baumannii*, and *A. nosocomialis* to grow on a given carbon source, overnight cultures grown in TSB in the case of *S. aureus* and *P. aeruginosa* or in LB Difco for *A. baumannii* and *A. nosocomialis* at 37°C were washed in M9 liquid medium without carbon source addition. Next, 1/100 dilutions were performed in M9 liquid medium supplemented with 5, 10, or 15 mM trehalose, phenylacetic acid (PAA), or acetoin as sole carbon sources or in TSB or LB as controls and grown stagnantly at 37°C under blue light or in the dark in 96-well microplates. At the indicated time points, the OD_{660} of the cultures was determined using an Epoch 2 microplate spectrophotometer (BioTek). Three independent experiments were performed, with each including three replicates for each strain and condition.

Desiccation assay. *A. nosocomialis* strain RUH2624 and *S. aureus* USA300 were grown overnight in 10 ml of LB or TSB, respectively, in the presence of blue light or in the dark at 37°C. Cells in stationary phase were centrifuged (5,000 rpm) and resuspended in sterile 0.9% NaCl. The bacterial concentration was adjusted to inoculate 1×10^7 CFU on each sample. After a 3-h starvation period, 20 μl of cell suspensions was spotted onto sterile cellulose filter paper pieces (Whatman; 1.5 cm by 1.5 cm), which had been previously sterilized by autoclaving. The membrane filters were placed in sterile petri dishes and incubated at 37°C under blue light or in the dark.

At each selected time point, filter paper pieces incubated under blue light or in the dark were located in tubes containing 1 ml of LB or TSB for *A. nosocomialis* or *S. aureus*, respectively, which were subsequently vortexed vigorously for 10 s. Vortexing was repeated after a 20-min incubation at 37°C and 200 rpm to remove the bacteria from the filter. Serial dilutions were prepared on 0.9% NaCl, plated onto LB agar or TSA plates, according to the microorganism, and then incubated at 37°C for 24 hours to finally determine CFU per milliliter. Three technical replicates were analyzed at each time point studied, and two and three independent experiments were performed for *S. aureus* and *A. nosocomialis*, respectively.

HaCaT cell infections. (i) Bacterial culture conditions. A total of 3 ml of TSB broth was inoculated with one fresh colony of *S. aureus* strain USA300, and the bacteria were grown in the presence of blue light or in the dark with shaking at 37°C for 24 hours. Then, a 1/100 dilution was performed in a new flask containing 3 ml of TSB broth, and the bacteria were further grown for another 2 hours, under the same conditions. Similar growth conditions were used for *Pseudomonas aeruginosa* PAO1 and PAE4840, with the exception that TSB was supplemented with 0.5% glucose (52). *A. baumannii* ATCC 19606 and *A. nosocomialis* RUH2624, as well as the *A. baumannii* ATCC 19606-derived mutant strains Δ*tssM* and Δ*blsA*, were grown in LB agar Difco plates for 18 hours at 37°C. A total of 3 ml of LB broth were inoculated with one fresh colony, and the bacteria were grown under static or shaking conditions for 24 hours in the presence of blue light or in the dark at 37°C. Then, 1/100 dilutions were performed in new flasks containing 3 ml of LB broth, and the bacteria were incubated for another 24 hours at 37°C, under the same conditions. When growing *A. baumannii* 19606 mutant strains, LB medium was supplemented with 30 μg/ml of Kn.

(ii) Eukaryotic cells and culture conditions. The well-established human keratinocyte cell line HaCaT was used throughout the study. HaCaT is a spontaneously transformed human epithelial cell line from adult skin, which maintains full epidermal differentiation capacity (43). HaCaT cells were grown routinely in DMEM high glucose (GibcoBRL, Gaithersburg, MD) supplemented with 10% fetal calf serum (FCS) (Life Technologies, Rockville, MD), 2 mM nonessential amino acids, and glutamine (GibcoBRL) at

37°C in 5% CO_2. In experiments in which different light conditions were used, HaCaT cells were first grown in the same classical DMEM for 24 hours in the dark. Then, immediately after infection, the keratinocyte culture was exposed to blue light or kept in the dark for the rest of the experiment. Uninfected HaCaT wells were included in every plate for all the experiments performed as viability controls and received the same light or dark treatments as the infection wells.

(iii) Bacterial adhesion and invasion assays. HaCaT cells were seeded at a density of 1.5×10^5 cells per well in 24-well culture plates harboring 500 μl of DMEM and incubated at 37°C in 5% CO_2 for 24 hours, until they formed 85% to 90% confluent cell monolayers. Bacteria were cultured for 3, 24, or 48 hours at 37°C in LB or TSB medium with or without shaking, as specified in "Bacterial culture conditions" above. Then, the bacteria were centrifuged, resuspended in DMEM, and added to the monolayers at an MOI of 100 or else specified. The plates were then centrifuged at 500 $\times$ *g* for 5 min at room temperature and incubated for 60 min at 37°C in 5% CO_2. For adhesion assays, the HaCaT cells were washed seven times with PBS to wash off nonadhered bacteria, and then the growing medium was replaced by 500 μl of fresh DMEM for the rest of the experiment. For the internalization assays, the HaCaT cells were washed three times with PBS and then incubated with growing medium supplemented with 100 μg ml^{-1} gentamicin for 90 min, in order to eliminate nonadherent and noninternalized bacteria. Then, the growing medium was replaced by 500 μl of DMEM with a gentamicin concentration of 10 μg ml^{-1} in the case of *S. aureus* or 200 μg ml^{-1} for *P. aeruginosa* for the remainder of the experiment. Immediately after infection, the culture plates were exposed to blue light or kept in the dark for the rest of the experiment (as indicated in "Bacterial culture conditions" above). Triplicate wells were included for each condition and time point studied. At least three independent experiments were performed for the infections with the different microorganisms. For bacterial counting, keratinocytes were lysed with 0.1% Triton X-100, and bacteria were recovered and enumerated after plating a dilution series onto TSB or LB agar at 2 and 24 hours postinfection. Dilutions covered the range from nondiluted to 10^{-5}, and for each dilution, the bacteria were quantified by triplicate for each condition and time point studied.

(iv) Keratinocyte viability. Cell viability was tested with the trypan blue exclusion method by counting viable cells using a Neubauer camera, after treatment of infected or noninfected HaCaT cultures with trypsin-EDTA (71). Briefly, the totality of cells (infected and noninfected) of each well was recovered after trypsin-EDTA treatment in 500 μl of PBS. Then, we performed a 1-to-10 dilution in PBS, and 10 μl of this solution was analyzed under the microscope using a Neubauer camera. Trypan blue is a dye derived from toluidine that has the ability to stain cells with loss of membrane integrity. Upon entry the cell, it binds to intracellular proteins, thereby rendering the cells a blue color. In contrast, undamaged cells are very selective concerning the compounds that pass through their membrane, effectively excluding this negatively charged dye. Therefore, the trypan blue exclusion assay allows one to directly identify and count viable (unstained) and dead (blue) cells in a given population under a microscope (71). The experiments were repeated at least 3 times, and each sample was quantified in triplicate. The results are expressed as the percentage of HaCaT survival, calculated as the number of viable cells at each light (L) or dark (D) condition and time point assayed, normalized to the number of cells in the uninfected control at time zero. For infections with *A. nosocomialis* and *A. baumannii*, keratinocyte viability was also determined by the MTT assay. Briefly, the MTT assay reports the metabolic status of eukaryotic cells, tested by a colorimetric assay based on the reduction of 3-(4,5-dimethyl-2-thiazolyl)-2,5-diphenyl-2H-tetrazolium bromide (MTT). MTT is taken up by the cells and reduced by the mitochondrial succinate dehydrogenase enzyme to its insoluble form, formazan. The ability of the cells to reduce MTT is, thus, an indicator of the integrity of the mitochondria and their functional activity and is interpreted as an indicator of cell viability. After the reduction to formazan, which is a violet crystal, this compound is released from the cells by solubilization with detergents, such as dimethyl sulfoxide (DMSO), and quantified by absorbance determination at 580 nm and 630 nm (71) (see the supplemental text and Fig. S7A to C).

Killing of *C. albicans* filaments. Assays were performed as described before (54), with the modification of incubating 1-ml cocultures without shaking at 37°C from 24 hours to 72 hours under dark or blue light conditions. Fungal CFU counts per milliliter were determined at each time point studied by plating convenient dilutions of the cocultures onto yeast extract-peptone-dextrose (YPD) agar containing 60 μg/ml tetracycline, 30 μg/ml chloramphenicol, and 30 μg/ml gentamicin, following incubation at 28°C for 48 h (54). These experiments were repeated at least three times using fresh samples each time.

SUPPLEMENTAL MATERIAL

Supplemental material is available online only.

SUPPLEMENTAL FILE 1, PDF file, 1.8 MB.

SUPPLEMENTAL FILE 2, XLSX file, 0.01 MB.

ACKNOWLEDGMENTS

We thank Gabriel Rabinovich for providing HaCaT cells and Daniela Gardiol for her advice and contributions to the experimental design. We thank Jovanka Voyich from Montana State University for providing the *hla* and complemented *hla* mutant. We kindly thank Dolores Campos for cell biology assistance and Lucas Daurelio for his help with statistical analyses.

This work was supported by grants from the Agencia Nacional de Promoción Científica y Tecnológica (PICT 2014-1161) and ASaCTeI (Ministerio de Ciencia, Tecnología e Innovación Productiva de la Provincia de Santa Fe) 2010-147-16 to M.A.M. and IO-021-18 to M.A.M. P.C., H.G., L.D., and M.A.M. are career investigators of CONICET. M.R.T. is a fellow from the same institution. We are also grateful to Wood-Whelan Research Fellowships from the International Union of Biochemistry and Molecular Biology for providing M.R.T. with a research travel grant to visit María Soledad Ramírez lab (CSUF, California), where some of the results shown here were obtained.

REFERENCES

1. Strachan CR, Davies J. 2017. The whys and wherefores of antibiotic resistance. Cold Spring Harb Perspect Med 7:a025171. https://doi.org/10.1101/cshperspect.a025171.
2. Mulani MS, Kamble EE, Kumkar SN, Tawre MS, Pardesi KR. 2019. Emerging strategies to combat ESKAPE pathogens in the era of antimicrobial resistance: a review. Front Microbiol 10:539. https://doi.org/10.3389/fmicb.2019.00539.
3. De Oliveira DMP, Forde BM, Kidd TJ, Harris PNA, Schembri MA, Beatson SA, Paterson DL, Walker MJ. 2020. Antimicrobial resistance in ESKAPE pathogens. Clin Microbiol Rev 33:e00181-19. https://doi.org/10.1128/CMR.00181-19.
4. Ma YX, Wang CY, Li YY, Li J, Wan QQ, Chen JH, Tay FR, Niu LN. 2020. Considerations and caveats in combating ESKAPE pathogens against nosocomial infections. Adv Sci (Weinh) 7:1901872. https://doi.org/10.1002/advs.201901872.
5. Rice LB. 2008. Federal funding for the study of antimicrobial resistance in nosocomial pathogens: no ESKAPE. J Infect Dis 197:1079–1081. https://doi.org/10.1086/533452.
6. Founou RC, Founou LL, Essack SY. 2017. Clinical and economic impact of antibiotic resistance in developing countries: a systematic review and meta-analysis. PLoS One 12:e0189621. https://doi.org/10.1371/journal.pone.0189621.
7. Oliveira A, Bleicher L, Schrago CG, Silva Junior FP. 2018. Conservation analysis and decomposition of residue correlation networks in the phospholipase A2 superfamily (PLA2s): insights into the structure-function relationships of snake venom toxins. Toxicon 146:50–60. https://doi.org/10.1016/j.toxicon.2018.03.013.
8. Pendleton JN, Gorman SP, Gilmore BF. 2013. Clinical relevance of the ESKAPE pathogens. Expert Rev Anti Infect Ther 11:297–308. https://doi.org/10.1586/eri.13.12.
9. Chaibenjawong P, Foster SJ. 2011. Desiccation tolerance in Staphylococcus aureus. Arch Microbiol 193:125–135. https://doi.org/10.1007/s00203-010-0653-x.
10. Mussi MA, Gaddy JA, Cabruja M, Arivett BA, Viale AM, Rasia R, Actis LA. 2010. The opportunistic human pathogen Acinetobacter baumannii senses and responds to light. J Bacteriol 192:6336–6345. https://doi.org/10.1128/JB.00917-10.
11. Muller GL, Tuttobene M, Altilio M, Martinez Amezaga M, Nguyen M, Cribb P, Cybulski LE, Ramirez MS, Altabe S, Mussi MA. 2017. Light modulates metabolic pathways and other novel physiological traits in the human pathogen Acinetobacter baumannii. J Bacteriol 199:e00011-17.https://doi.org/10.1128/JB.00011-17.
12. Pezza A, Tuttobene M, Abatedaga I, Valle L, Borsarelli CD, Mussi MA. 2019. Through the eyes of a pathogen: light perception and signal transduction in Acinetobacter baumannii. Photochem Photobiol Sci 18:2363–2373. https://doi.org/10.1039/c9pp00261h.
13. Ramirez MS, Muller GL, Perez JF, Golic AE, Mussi MA. 2015. More than just light: clinical relevance of light perception in the nosocomial pathogen Acinetobacter baumannii and other members of the genus Acinetobacter. Photochem Photobiol 91:1291–1301. https://doi.org/10.1111/php.12523.
14. Ramirez MS, Traglia GM, Perez JF, Muller GL, Martinez MF, Golic AE, Mussi MA. 2015. White and blue light induce reduction in susceptibility to minocycline and tigecycline in Acinetobacter spp. and other bacteria of clinical importance. J Med Microbiol 64:525–537. https://doi.org/10.1099/jmm.0.000048.
15. Tuttobene MR, Cribb P, Mussi MA. 2018. BlsA integrates light and temperature signals into iron metabolism through Fur in the human pathogen Acinetobacter baumannii. Sci Rep 8:7728. https://doi.org/10.1038/s41598-018-26127-8.
16. Tuttobene MR, Fernandez-Garcia L, Blasco L, Cribb P, Ambroa A, Muller GL, Fernandez-Cuenca F, Bleriot I, Rodriguez RE, Barbosa BGV, Lopez-Rojas R, Trastoy R, Lopez M, Bou G, Tomas M, Mussi MA. 2019. Quorum and light signals modulate acetoin/butanediol catabolism in Acinetobacter spp. Front Microbiol 10:1376. https://doi.org/10.3389/fmicb.2019.01376.
17. Abatedaga I, Valle L, Golic AE, Muller GL, Cabruja M, Moran Vieyra FE, Jaime PC, Mussi MA, Borsarelli CD. 2017. Integration of temperature and blue-light sensing in Acinetobacter baumannii through the BlsA sensor. Photochem Photobiol 93:805–814. https://doi.org/10.1111/php.12760.
18. Golic AE, Valle L, Jaime PC, Alvarez CE, Parodi C, Borsarelli CD, Abatedaga I, Mussi MA. 2019. BlsA is a low to moderate temperature blue light photoreceptor in the human pathogen Acinetobacter baumannii. Front Microbiol 10:1925. https://doi.org/10.3389/fmicb.2019.01925.
19. Golic A, Vaneechoutte M, Nemec A, Viale AM, Actis LA, Mussi MA. 2013. Staring at the cold sun: blue light regulation is distributed within the genus Acinetobacter. PLoS One 8:e55059. https://doi.org/10.1371/journal.pone.0055059.
20. Nemec A, Krizova L, Maixnerova M, van der Reijden TJ, Deschaght P, Passet V, Vaneechoutte M, Brisse S, Dijkshoorn L. 2011. Genotypic and phenotypic characterization of the Acinetobacter calcoaceticus-Acinetobacter baumannii complex with the proposal of Acinetobacter pittii sp. nov. (formerly Acinetobacter genomic species 3) and Acinetobacter nosocomialis sp. nov. (formerly Acinetobacter genomic species 13TU). Res Microbiol 162:393–404. https://doi.org/10.1016/j.resmic.2011.02.006.
21. Schleicher X, Higgins PG, Wisplinghoff H, Korber-Irrgang B, Kresken M, Seifert H. 2013. Molecular epidemiology of Acinetobacter baumannii and Acinetobacter nosocomialis in Germany over a 5-year period (2005–2009). Clin Microbiol Infect 19:737–742. https://doi.org/10.1111/1469-0691.12026.
22. Vandenesch F, Lina G, Henry T. 2012. Staphylococcus aureus hemolysins, bi-component leukocidins, and cytolytic peptides: a redundant arsenal of membrane-damaging virulence factors? Front Cell Infect Microbiol 2:12. https://doi.org/10.3389/fcimb.2012.00012.
23. Cerqueira GM, Kostoulias X, Khoo C, Aibinu I, Qu Y, Traven A, Peleg AY. 2014. A global virulence regulator in Acinetobacter baumannii and its control of the phenylacetic acid catabolic pathway. J Infect Dis 210:46–55. https://doi.org/10.1093/infdis/jiu024.
24. Nair D, Memmi G, Hernandez D, Bard J, Beaume M, Gill S, Francois P, Cheung AL. 2011. Whole-genome sequencing of Staphylococcus aureus strain RN4220, a key laboratory strain used in virulence research, identifies mutations that affect not only virulence factors but also the fitness of the strain. J Bacteriol 193:2332–2335. https://doi.org/10.1128/JB.00027-11.
25. Tenover FC, Goering RV. 2009. Methicillin-resistant Staphylococcus aureus strain USA300: origin and epidemiology. J Antimicrob Chemother 64:441–446. https://doi.org/10.1093/jac/dkp241.
26. Nygaard TK, Pallister KB, DuMont AL, DeWald M, Watkins RL, Pallister EQ, Malone C, Griffith S, Horswill AR, Torres VJ, Voyich JM. 2012. Alpha-toxin induces programmed cell death of human T cells, B cells, and monocytes during USA300 infection. PLoS One 7:e36532. https://doi.org/10.1371/journal.pone.0036532.
27. Malone CL, Boles BR, Lauderdale KJ, Thoendel M, Kavanaugh JS, Horswill AR. 2009. Fluorescent reporters for Staphylococcus aureus. J Microbiol Methods 77:251–260. https://doi.org/10.1016/j.mimet.2009.02.011.
28. Goerke C, Fluckiger U, Steinhuber A, Zimmerli W, Wolz C. 2001. Impact of the regulatory loci agr, sarA and sae of Staphylococcus aureus on the induction of alpha-toxin during device-related infection resolved by

direct quantitative transcript analysis. Mol Microbiol 40:1439–1447. https://doi.org/10.1046/j.1365-2958.2001.02494.x.
29. Zimbler DL, Penwell WF, Gaddy JA, Menke SM, Tomaras AP, Connerly PL, Actis LA. 2009. Iron acquisition functions expressed by the human pathogen Acinetobacter baumannii. Biometals 22:23–32. https://doi.org/10.1007/s10534-008-9202-3.
30. Bhuiyan MS, Ellett F, Murray GL, Kostoulias X, Cerqueira GM, Schulze KE, Mahamad Maifiah MH, Li J, Creek DJ, Lieschke GJ, Peleg AY. 2016. Acinetobacter baumannii phenylacetic acid metabolism influences infection outcome through a direct effect on neutrophil chemotaxis. Proc Natl Acad Sci U S A 113:9599–9604. https://doi.org/10.1073/pnas.1523116113.
31. Audrain B, Letoffe S, Ghigo J-M. 2015. Airborne bacterial interactions: functions out of thin air? Front Microbiol 6:1476. https://doi.org/10.3389/fmicb.2015.01476.
32. Diacovich L, Lorenzi L, Tomassetti M, Meresse S, Gramajo H. 2017. The infectious intracellular lifestyle of Salmonella enterica relies on the adaptation to nutritional conditions within the Salmonella-containing vacuole. Virulence 8:975–992. https://doi.org/10.1080/21505594.2016.1270493.
33. Piazza A, Zimaro T, Garavaglia BS, Ficarra FA, Thomas L, Marondedze C, Feil R, Lunn JE, Gehring C, Ottado J, Gottig N. 2015. The dual nature of trehalose in citrus canker disease: a virulence factor for Xanthomonas citri subsp. citri and a trigger for plant defence responses. J Exp Bot 66:2795–2811. https://doi.org/10.1093/jxb/erv095.
34. Freeman BC, Chen C, Beattie GA. 2010. Identification of the trehalose biosynthetic loci of Pseudomonas syringae and their contribution to fitness in the phyllosphere. Environ Microbiol 12:1486–1497. https://doi.org/10.1111/j.1462-2920.2010.02171.x.
35. Djonovic S, Urbach JM, Drenkard E, Bush J, Feinbaum R, Ausubel JL, Traficante D, Risech M, Kocks C, Fischbach MA, Priebe GP, Ausubel FM. 2013. Trehalose biosynthesis promotes Pseudomonas aeruginosa pathogenicity in plants. PLoS Pathog 9:e1003217. https://doi.org/10.1371/journal.ppat.1003217.
36. Woodruff PJ, Carlson BL, Siridechadilok B, Pratt MR, Senaratne RH, Mougous JD, Riley LW, Williams SJ, Bertozzi CR. 2004. Trehalose is required for growth of Mycobacterium smegmatis. J Biol Chem 279:28835–28843. https://doi.org/10.1074/jbc.M313103200.
37. Zeidler S, Müller V. 2019. The role of compatible solutes in desiccation resistance of Acinetobacter baumannii. Microbiologyopen 8:e00740. https://doi.org/10.1002/mbo3.740.
38. Crowe JH, Oliver AE, Tablin F. 2002. Is there a single biochemical adaptation to anhydrobiosis? Integr Comp Biol 42:497–503. https://doi.org/10.1093/icb/42.3.497.
39. Tapia H, Koshland DE. 2014. Trehalose is a versatile and long-lived chaperone for desiccation tolerance. Curr Biol 24:2758–2766. https://doi.org/10.1016/j.cub.2014.10.005.
40. Denton M, Wilcox MH, Parnell P, Green D, Keer V, Hawkey PM, Evans I, Murphy P. 2004. Role of environmental cleaning in controlling an outbreak of Acinetobacter baumannii on a neurosurgical intensive care unit. J Hosp Infect 56:106–110. https://doi.org/10.1016/j.jhin.2003.10.017.
41. Jawad A, Snelling AM, Heritage J, Hawkey PM. 1998. Exceptional desiccation tolerance of Acinetobacter radioresistens. J Hosp Infect 39:235–240. https://doi.org/10.1016/s0195-6701(98)90263-8.
42. Fournier PE, Richet H. 2006. The epidemiology and control of Acinetobacter baumannii in health care facilities. Clin Infect Dis 42:692–699. https://doi.org/10.1086/500202.
43. Boukamp P, Petrussevska RT, Breitkreutz D, Hornung J, Markham A, Fusenig NE. 1988. Normal keratinization in a spontaneously immortalized aneuploid human keratinocyte cell line. J Cell Biol 106:761–771. https://doi.org/10.1083/jcb.106.3.761.
44. Morgene MF, Maurin C, Pillet S, Berthelot P, Morfin F, Pozzetto B, Botelho-Nevers E, Verhoeven PO. 2018. HaCaT epithelial cells as an innovative novel model of rhinovirus infection and impact of clarithromycin treatment on infection kinetics. Virology 523:27–34. https://doi.org/10.1016/j.virol.2018.07.025.
45. Tribelli PM, Luqman A, Nguyen MT, Madlung J, Fan S-H, Macek B, Sass P, Bitschar K, Schittek B, Kretschmer D, Götz F. 2020. Staphylococcus aureus Lpl protein triggers human host cell invasion via activation of Hsp90 receptor. Cell Microbiol 22:e13111. https://doi.org/10.1111/cmi.13111.
46. Jordana-Lluch E, Garcia V, Kingdon ADH, Singh N, Alexander C, Williams P, Hardie KR. 2020. A simple polymicrobial biofilm keratinocyte colonization model for exploring interactions between commensals, pathogens and antimicrobials. Front Microbiol 11:291. https://doi.org/10.3389/fmicb.2020.00291.
47. Gupta S, Tang C, Tran M, Kadouri DE. 2016. Effect of predatory bacteria on human cell lines. PLoS One 11:e0161242. https://doi.org/10.1371/journal.pone.0161242.
48. Hoesl C, Zanuttigh E, Frohlich T, Philippou-Massier J, Krebs S, Blum H, Dahlhoff M. 2020. The secretome of skin cancer cells activates the mTOR/MYC pathway in healthy keratinocytes and induces tumorigenic properties. Biochim Biophys Acta Mol Cell Res 1867:118717. https://doi.org/10.1016/j.bbamcr.2020.118717.
49. Mempel M, Schnopp C, Hojka M, Fesq H, Weidinger S, Schaller M, Korting HC, Ring J, Abeck D. 2002. Invasion of human keratinocytes by Staphylococcus aureus and intracellular bacterial persistence represent haemolysin-independent virulence mechanisms that are followed by features of necrotic and apoptotic keratinocyte cell death. Br J Dermatol 146:943–951. https://doi.org/10.1046/j.1365-2133.2002.04752.x.
50. Soong G, Chun J, Parker D, Prince A. 2012. Staphylococcus aureus activation of caspase 1/calpain signaling mediates invasion through human keratinocytes. J Infect Dis 205:1571–1579. https://doi.org/10.1093/infdis/jis244.
51. Kroken AR, Chen CK, Evans DJ, Yahr TL, Fleiszig SMJ. 2018. The impact of ExoS on Pseudomonas aeruginosa internalization by epithelial cells is independent of fleQ and correlates with bistability of type three secretion system gene expression. mBio 9:e00668-18.https://doi.org/10.1128/mBio.00668-18.
52. Hosseinidoust Z, van de Ven TG, Tufenkji N. 2013. Evolution of Pseudomonas aeruginosa virulence as a result of phage predation. Appl Environ Microbiol 79:6110–6116. https://doi.org/10.1128/AEM.01421-13.
53. Holloway BW, Römling U, Tümmler B. 1994. Genomic mapping of Pseudomonas aeruginosa PAO. Microbiology (Reading) 140:2907–2929. https://doi.org/10.1099/13500872-140-11-2907.
54. Gaddy JA, Tomaras AP, Actis LA. 2009. The Acinetobacter baumannii 19606 OmpA protein plays a role in biofilm formation on abiotic surfaces and in the interaction of this pathogen with eukaryotic cells. Infect Immun 77:3150–3160. https://doi.org/10.1128/IAI.00096-09.
55. Bentancor LV, Routray A, Bozkurt-Guzel C, Camacho-Peiro A, Pier GB, Maira-Litrán T. 2012. Evaluation of the trimeric autotransporter Ata as a vaccine candidate against Acinetobacter baumannii infections. Infect Immun 80:3381–3388. https://doi.org/10.1128/IAI.06096-11.
56. Weber BS, Ly PM, Irwin JN, Pukatzki S, Feldman MF. 2015. A multidrug resistance plasmid contains the molecular switch for type VI secretion in Acinetobacter baumannii. Proc Natl Acad Sci U S A 112:9442–9447. https://doi.org/10.1073/pnas.1502966112.
57. Repizo GD, Gagné S, Foucault-Grunenwald ML, Borges V, Charpentier X, Limansky AS, Gomes JP, Viale AM, Salcedo SP. 2015. Differential role of the T6SS in Acinetobacter baumannii virulence. PLoS One 10:e0138265. https://doi.org/10.1371/journal.pone.0138265.
58. Liao Y-T, Kuo S-C, Lee Y-T, Chen C-P, Lin S-W, Shen L-J, Fung C-P, Cho W-L, Chen T-L. 2014. Sheltering effect and indirect pathogenesis of carbapenem-resistant Acinetobacter baumannii in polymicrobial infection. Antimicrob Agents Chemother 58:3983–3990. https://doi.org/10.1128/AAC.02636-13.
59. Dhamgaye S, Qu Y, Peleg AY. 2016. Polymicrobial infections involving clinically relevant Gram-negative bacteria and fungi. Cell Microbiol 18:1716–1722. https://doi.org/10.1111/cmi.12674.
60. Hammer ND, Skaar EP. 2011. Molecular mechanisms of Staphylococcus aureus iron acquisition. Annu Rev Microbiol 65:129–147. https://doi.org/10.1146/annurev-micro-090110-102851.
61. Chapartegui-González I, Lázaro-Díez M, Bravo Z, Navas J, Icardo JM, Ramos-Vivas J. 2018. Acinetobacter baumannii maintains its virulence after long-time starvation. PLoS One 13:e0201961. https://doi.org/10.1371/journal.pone.0201961.
62. Nakonieczna J, Wozniak A, Pieranski M, Rapacka-Zdonczyk A, Ogonowska P, Grinholc M. 2019. Photoinactivation of ESKAPE pathogens: overview of novel therapeutic strategy. Future Med Chem 11:443–461. https://doi.org/10.4155/fmc-2018-0329.
63. Wang Y, Harrington OD, Wang Y, Murray CK, Hamblin MR, Dai T. 2017. In vivo investigation of antimicrobial blue light therapy for multidrug-resistant Acinetobacter baumannii burn infections using bioluminescence imaging. J Vis Exp https://doi.org/10.3791/54997.
64. Amin RM, Bhayana B, Hamblin MR, Dai T. 2016. Antimicrobial blue light inactivation of Pseudomonas aeruginosa by photo-excitation of endogenous porphyrins: in vitro and in vivo studies. Lasers Surg Med 48:562–568. https://doi.org/10.1002/lsm.22474.
65. Katayama B, Ozawa T, Morimoto K, Awazu K, Ito N, Honda N, Oiso N, Tsuruta D. 2018. Enhanced sterilization and healing of cutaneous pseudomonas infection using 5-aminolevulinic acid as a photosensitizer with

410-nm LED light. J Dermatol Sci 90:323–331. https://doi.org/10.1016/j.jdermsci.2018.03.001.
66. Mukherjee S, Jemielita M, Stergioula V, Tikhonov M, Bassler BL. 2019. Photosensing and quorum sensing are integrated to control Pseudomonas aeruginosa collective behaviors. PLoS Biol 17:e3000579. https://doi.org/10.1371/journal.pbio.3000579.
67. Kahl LJ, Price-Whelan A, Dietrich LEP. 2020. Light-mediated decreases in cyclic di-GMP levels inhibit structure formation in Pseudomonas aeruginosa biofilms. J Bacteriol 202:e00117-20.https://doi.org/10.1128/JB.00117-20.
68. Wood CR, Ohneck EJ, Edelmann RE, Actis LA. 2018. A light-regulated type I pilus contributes to Acinetobacter baumannii biofilm, motility, and virulence functions. Infect Immun 86:e00442-18. https://doi.org/10.1128/IAI.00442-18.
69. Magiorakos AP, Srinivasan A, Carey RB, Carmeli Y, Falagas ME, Giske CG, Harbarth S, Hindler JF, Kahlmeter G, Olsson-Liljequist B, Paterson DL, Rice LB, Stelling J, Struelens MJ, Vatopoulos A, Weber JT, Monnet DL. 2012. Multidrug-resistant, extensively drug-resistant and pandrug-resistant bacteria: an international expert proposal for interim standard definitions for acquired resistance. Clin Microbiol Infect 18:268–281. https://doi.org/10.1111/j.1469-0691.2011.03570.x.
70. Traglia G, Chiem K, Quinn B, Fernandez JS, Montaña S, Almuzara M, Mussi MA, Tolmasky ME, Iriarte A, Centrón D, Ramírez MS. 2018. Genome sequence analysis of an extensively drug-resistant Acinetobacter baumannii indigo-pigmented strain depicts evidence of increase genome plasticity. Sci Rep 8:16961. https://doi.org/10.1038/s41598-018-35377-5.
71. Strober W. 2015. Trypan blue exclusion test of cell viability. Curr Protoc Immunol 111:A3.B.1–A3.B.3.